

FIBER-OPTIC COMMUNICATIONS

22.1 COMPONENTS OF THE OPTICAL FIBER LINK

- A. Optical Fibers
- B. Sources for Optical Transmitters
- C. Detectors for Optical Receivers
- D. Fiber-Optic Systems

22.2 MODULATION, MULTIPLEXING, AND COUPLING

- A. Modulation
- B. Multiplexing
- C. Couplers

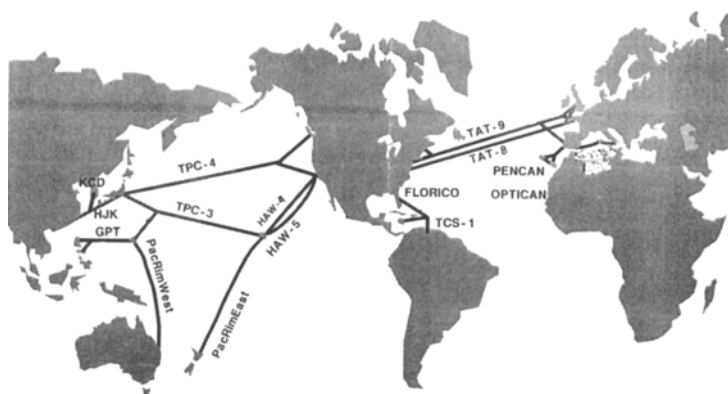
22.3 SYSTEM PERFORMANCE

- A. Digital Communication System
- B. Analog Communication System


22.4 RECEIVER SENSITIVITY

22.5 COHERENT OPTICAL COMMUNICATIONS

- A. Heterodyne Detection
- B. Performance of the Analog Heterodyne Receiver
- C. Performance of the Digital Heterodyne Receiver
- D. Coherent Systems



AT&T undersea fiber-optic communication network of the 1990s



Until recently, virtually all communication systems have relied on the transmission of information over electrical cables or have made use of radio-frequency and microwave electromagnetic radiation propagating in free space. It would appear that the use of light would have been a more natural choice for communications since, unlike electricity and radio waves, it did not have to be discovered. The reasons for the delay in the development of this technology are twofold: the difficulty of producing a light source that could be rapidly switched on and off and therefore could encode information at a high rate, and the fact that light is easily obstructed by opaque objects such as clouds, fog, smoke, and haze. Unlike radio-frequency and microwave radiation, light is rarely suitable for free-space communication.

Lightwave communications has recently come into its own, however, and indeed it is now the preferred technology in many applications. It is used for the transmission of voice, data, telemetry, and video in long-distance and local-area networks, and is suitable for a great diversity of other applications (e.g., cable television). Lightwave technology affords the user enormous transmission capacity, distant spacings of repeaters, immunity from electromagnetic interference, and relative ease of installation.

The spectacular successes of fiber-optic communications have their roots in two critical photonic inventions: the development of the light-emitting diode (LED) and the development of the low-loss optical fiber as a light conduit. Suitable detectors of light have been available for some time, although their performance has been improved dramatically in recent years. Interest in optical communications was initially stirred by the invention of the laser in the early 1960s. However, the first generation of fiber-optic communication systems made use of LED sources and indeed many present local-area commercial systems continue to do so. Nevertheless, most lightwave communication systems (such as long-haul single-mode fiber-optic systems and short-haul free-space systems) do benefit from the large optical power, narrow linewidth, and high directivity provided by the laser. The proposed extension of the fiber network to reach individual dwellings will rely on the use of diode lasers.

A fiber-optic communication system comprises three basic elements: a compact light source, a low-loss/low-dispersion optical fiber, and a photodetector. These optical components have been discussed in Chaps. 16, 8, and 17, respectively. In this chapter we examine their role in the context of the overall design, operation, and performance of an optical communication link. Optical accessories such as connectors, couplers, switches, and multiplexing devices, as well as splices, are also essential to the successful operation of fiber links and networks. Optical-fiber amplifiers have also proved themselves to be very valuable adjuncts to such systems. The principles of some of these devices have been discussed in Chap. 21 and in other parts of this book.

Although the waveguiding properties of different types of optical fibers have been discussed in detail in Chap. 8, this material is reviewed in Sec. 22.1 (in abbreviated form) to make this chapter self-contained. A brief summary of the properties of semiconductor photon sources and detectors suitable for fiber-optic communication systems is also provided in this section. This is followed, in Sec. 22.2, by an introduction to modulation, multiplexing, and coupling systems used in fiber-optic communications.

Section 22.3 introduces the basic design principles applicable to long-distance digital and analog fiber-optic communication systems. The maximum fiber length that can be used to transmit data (at a given rate and with a prescribed level of performance) is determined. Performance deteriorates if the data rate exceeds the fiber bandwidth, or if the received power is smaller than the receiver sensitivity (so that the signal cannot be distinguished from noise). The sensitivity of an optical receiver operating in a binary digital communication mode is evaluated in Sec. 22.4. It is of interest to compare these results with the sensitivity of an analog optical receiver, which was determined in Sec. 17.5D.

Coherent optical communication systems, which are introduced in Sec. 22.5, use light not as a source of controllable power but rather as an electromagnetic wave of controllable amplitude, phase, or frequency. Coherent optical systems are the natural extension to higher frequencies of conventional radio and microwave communications. They provide substantial gains in receiver sensitivity, permitting further spacings between repeaters and increased data rates.

22.1 COMPONENTS OF THE OPTICAL FIBER LINK

A. Optical Fibers

An optical fiber is a cylindrical dielectric waveguide made of low-loss materials, usually fused silica glass of high chemical purity. The core of the waveguide has a refractive index slightly higher than that of the outer medium, the cladding, so that light is guided along the fiber axis by total internal reflection. As described in Chap. 8, the transmission of light through the fiber may be studied by examining the trajectories of rays within the core. A more complete analysis makes use of electromagnetic theory. Light waves travel in the fiber in the form of modes, each with a distinct spatial distribution, polarization, propagation constant, group velocity, and attenuation coefficient. There is, however, a correspondence between each mode and a ray that bounces within the core in a distinct trajectory.

Step-Index Fibers

In a step-index fiber, the refractive index is n_1 in the core and abruptly decreases to n_2 in the cladding [Fig. 22.1-1(a)]. The fractional refractive index change $\Delta = (n_1 - n_2)/n_1$ is usually very small ($\Delta = 0.001$ to 0.02). Light rays making angles with the fiber axis smaller than the complement of the critical angle, $\bar{\theta}_c = \cos^{-1}(n_2/n_1)$, are guided within the core by multiple total internal reflections at the core-cladding boundary. The angle $\bar{\theta}_c$ in the fiber corresponds to an angle θ_a for rays incident from air into the fiber, where $\sin \theta_a = \text{NA}$ and $\text{NA} = (n_1^2 - n_2^2)^{1/2} \approx n_1(2\Delta)^{1/2}$ is called the numerical aperture. θ_a is the acceptance angle of the fiber.

The number of guided modes M is governed by the fiber V parameter, $V = 2\pi(a/\lambda_o)\text{NA}$, where a/λ_o is the ratio of the core radius a to the wavelength λ_o . In a fiber with $V \gg 1$, there are a large number of modes, $M \approx V^2/2$, and the minimum and maximum group velocities of the modes are $v_{\min} \approx c_1(1 - \Delta) = c_1(n_2/n_1)$ and $v_{\max} \approx c_1 = c_o/n_1$. When an impulse of light travels a distance L in the fiber, it undergoes different time delays, spreading over a time interval $2\sigma_\tau = L/c_1(1 - \Delta) - L/c_1 \approx (L/c_1)\Delta$. The result is a pulse of rms width

$$\sigma_\tau \approx \frac{L}{2c_1} \Delta.$$

(22.1-1)

Fiber Response Time
(Multimode Step-Index Fiber)

The overall pulse width is therefore proportional to the fiber length L and to the fractional refractive index change Δ . This effect is called **modal dispersion**.

Graded-Index Fibers

In a graded-index fiber, the refractive index of the core varies gradually from a maximum value n_1 on the fiber axis to a minimum value n_2 at the core-cladding boundary [Fig. 22.1-1(b)]. The fractional refractive index change $\Delta = (n_1 - n_2)/n_1 \ll 1$. Rays follow curved trajectories, with paths shorter than those in the step-index fiber. The axial ray travels the shortest distance at the smallest phase velocity (largest refractive index), whereas oblique rays travel longer distances at higher phase velocities (smaller refractive indices), so that the delay times are equalized. The maximum difference between the group velocities of the modes is therefore much smaller than in the step-index fiber.

When the fiber is graded optimally (using an approximately parabolic profile), the modes travel with almost equal group velocities. When the fiber V parameter, $V = 2\pi(a/\lambda_o)NA$, is large, the number of modes $M \approx V^2/4$; i.e., there are approximately half as many modes as in a step-index fiber with the same value of V . The group velocities then range between c_1 and $c_1(1 - \Delta^2/2)$, so that for a fiber of length L an input impulse of light spreads to a width

$$\sigma_\tau \approx \frac{L}{4c_1} \Delta^2.$$

(22.1-2)

Fiber Response Time
(Graded-Index Fiber;
Parabolic Profile)

This is a factor $\Delta/2$ smaller than in the equivalent step-index fiber. This reduction factor, however, is usually not fully met in practical graded-index fibers because of the difficulty of achieving ideal index profiles.

Single-Mode Fibers

When the core radius a and the numerical aperture NA of a step-index fiber are sufficiently small so that $V < 2.405$ (the smallest root of the Bessel function J_0), only a single mode is allowed. One advantage of using a single-mode fiber is the elimination of pulse spreading caused by modal dispersion. Pulse spreading occurs, nevertheless, since the initial pulse has a finite spectral linewidth and since the group velocities (and therefore the delay times) are wavelength dependent. This effect is called **chromatic dispersion**. There are two origins of chromatic dispersion: **material dispersion**, which results from the dependence of the refractive index on the wavelength, and **waveguide dispersion**, which is a consequence of the dependence of the group velocity of each mode on the ratio between the core radius and the wavelength. Material dispersion is usually larger than waveguide dispersion.

A short optical pulse of spectral width σ_λ spreads to a temporal width

$$\sigma_\tau = |D|\sigma_\lambda L,$$

(22.1-3)

Fiber Response Time
(Material Dispersion)

proportional to the propagation distance L (km) and to the source linewidth σ_λ (nm), where D is the dispersion coefficient (ps/km-nm). The parameter D involves a combination of material and waveguide dispersion. For weakly guiding fibers ($\Delta \ll 1$), D may be separated into a sum $D_\lambda + D_w$ of the material and waveguide contributions. The geometries, refractive-index profiles, and pulse broadening in multimode step-

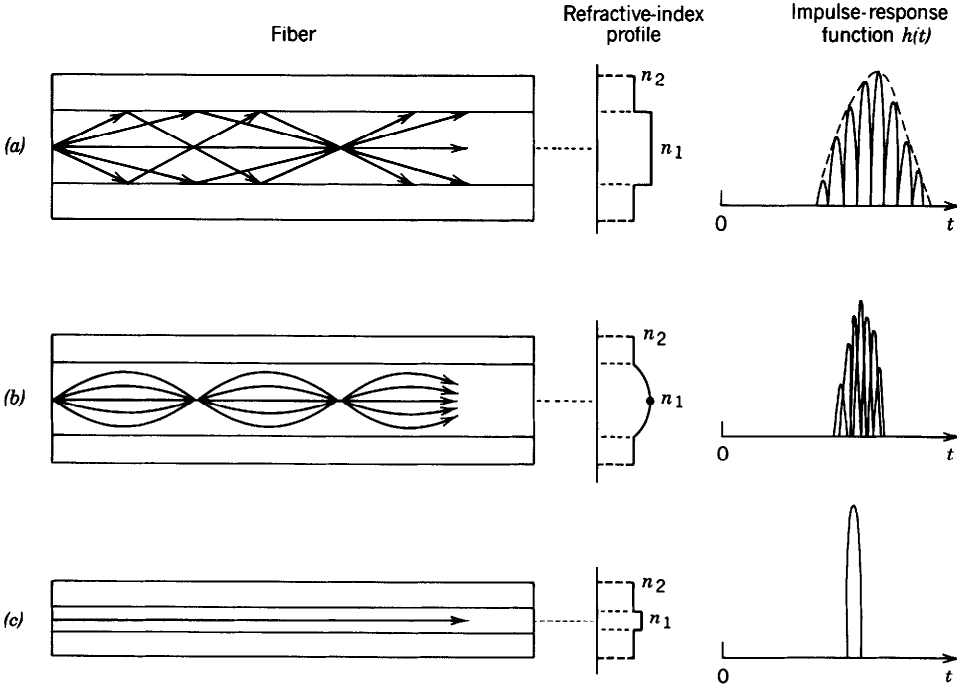


Figure 22.1-1 (a) Multimode step-index fibers: relatively large core diameter; uniform refractive indices in the core and cladding; large pulse spreading due to modal dispersion. (b) Graded-index fibers: refractive index of the core is graded; there are fewer modes; pulse broadening due to modal dispersion is reduced. (c) Single-mode fibers: small core diameter; no modal dispersion; pulse broadening is due only to material and waveguide dispersion.

index and graded-index fibers and in single-mode fibers are schematically compared in Fig. 22.1-1.

Material Attenuation and Dispersion

The wavelength dependence of the attenuation coefficients of different types of fused-silica-glass fibers are illustrated in Fig. 22.1-2. As the wavelength increases beyond the visible band, the attenuation drops to a minimum of approximately 0.3 dB/km at $\lambda_o = 1.3 \mu\text{m}$, increases slightly at $1.4 \mu\text{m}$ because of OH-ion absorption, and then drops again to its absolute minimum of $\approx 0.16 \text{ dB/km}$ at $\lambda_o = 1.55 \mu\text{m}$, beyond which it rises sharply. The dispersion coefficient D_λ of fused silica glass is also wavelength dependent, as illustrated in Fig. 22.1-2. It is zero at $\lambda_o \approx 1.312 \mu\text{m}$.

Operating Wavelengths for Fiber-Optic Communications

As illustrated in Fig. 22.1-2, the minimum attenuation occurs at $\approx 1.55 \mu\text{m}$, whereas the minimum material dispersion occurs at $\approx 1.312 \mu\text{m}$. The choice between these two wavelengths depends on the relative importance of power loss versus pulse spreading, as explained in Sec. 22.3. However, the availability of an appropriate light source is also a factor. First-generation fiber-optic communication systems operated at $\approx 0.87 \mu\text{m}$ (the wavelength of AlGaAs light-emitting diodes and diode lasers), where both attenuation and material dispersion are relatively high. More advanced systems operate at 1.3 and $1.55 \mu\text{m}$. A summary of the salient properties of silica-glass fibers at these three operating wavelengths is provided in Table 22.1-1.

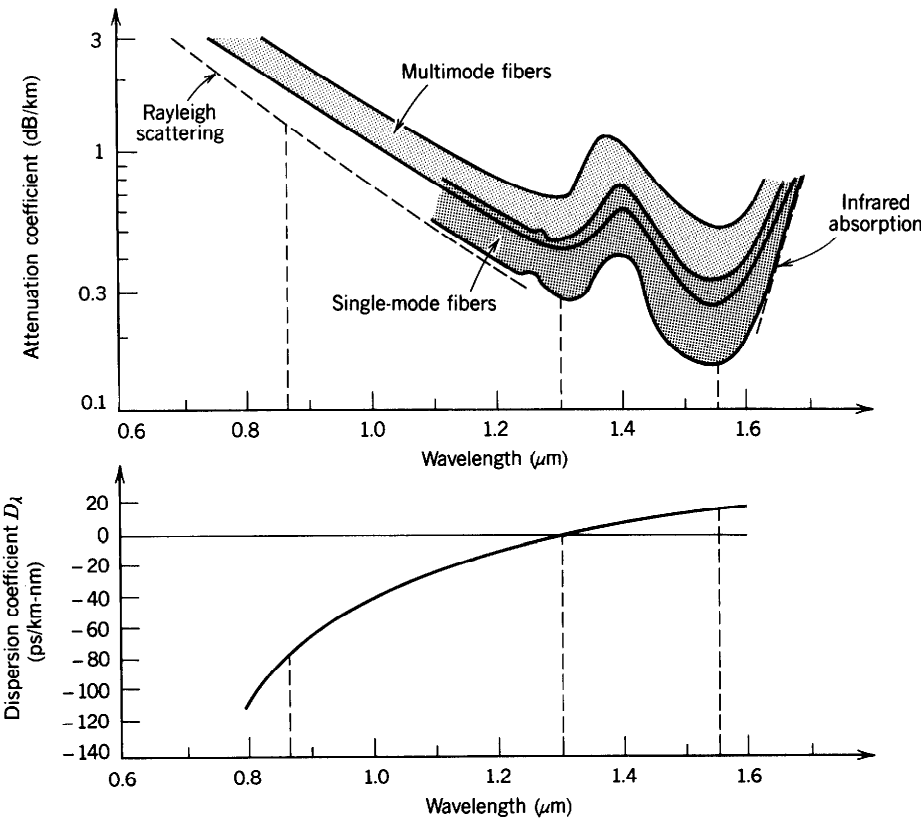


Figure 22.1-2 Wavelength dependence of the attenuation and material dispersion coefficients of silica-glass fibers, indicating three wavelengths at which fiber-optic communication systems typically operate: 0.87, 1.3, and 1.55 μm .

Advanced designs using graded-index single-mode fibers aim at balancing waveguide dispersion with material dispersion, so that the overall dispersion coefficient vanishes at $\lambda_o = 1.55 \mu\text{m}$ rather than at 1.312 μm . This is achieved at the expense of a slight increase of the attenuation coefficient.

Transfer Function, Response Time, and Bandwidth

A communication channel is usually characterized by its impulse-response function $h(t)$. For the fiber-optic channel, this is the received power as a function of time when the input power at the transmitter side is an impulse function $\delta(t)$ [see Figs. 22.1-3(a) and 22.1-1]. An equivalent function that also characterizes the channel is the transfer function $\mathcal{H}(f)$. This is obtained, as illustrated in Fig. 22.1-3(b), by modulating the

TABLE 22.1-1 Minimum Attenuation and Material Dispersion Coefficients of Silica-Glass Fiber at Three Wavelengths^a

$\lambda_o (\mu\text{m})$	Attenuation (dB/km)	Dispersion (ps/km-nm)
0.87	1.5	−80
1.312	0.3	0
1.55	0.16	+17

^aActual values depend on the type of fiber and the dopants used.

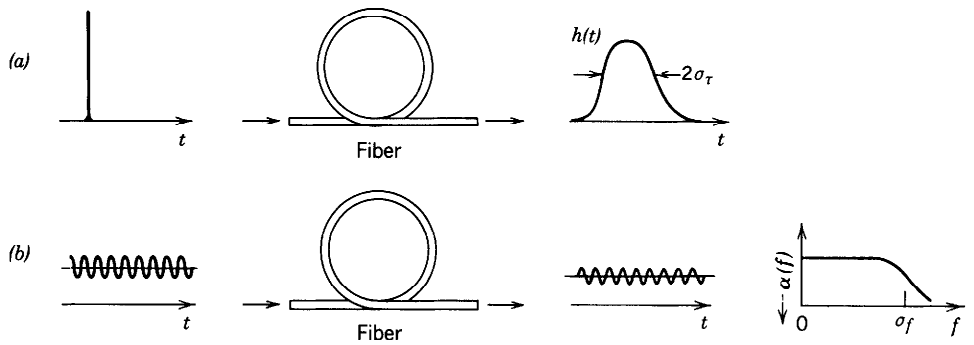


Figure 22.1-3 (a) Measurement of the impulse-response function $h(t)$. (b) Measurement of the transfer function $\mathcal{H}(f)$. The attenuation coefficient $\alpha(f)$ is the negative of the absolute value of $\mathcal{H}(f)$ in dB units for $L = 1$ km.

input power ($P(z)$ at $z = 0$) sinusoidally at frequency f , $P(0) = P_0(0) + P_s(0) \cos(2\pi ft)$, where $P_s(0) < P_0(0)$, and measuring the output power after propagation a distance L through the fiber, $P(L) = P_0(L) + P_s(L) \cos(2\pi ft + \varphi)$. The transfer function is $\mathcal{H}(f) = [P_s(L)/P_s(0)] \exp(j\varphi)$. Clearly, $P_0(L) = \mathcal{H}(0)P_0(0)$, where $\mathcal{H}(0)$ is the transmittance \mathcal{T} .

The absolute value $|\mathcal{H}(f)|$ is the factor by which the amplitude of the modulated signal at frequency f is reduced as a result of propagation. The attenuation coefficient $\alpha(f)$ is defined by

$$\alpha(f) = \frac{-10 \log_{10}(|\mathcal{H}(f)|)}{L}$$

(22.1-4)

Fiber Attenuation Coefficient
(dB/km) at Modulation
Frequency f

and has units of dB/km. Thus $|\mathcal{H}(f)| = \exp[-\alpha(f)L]$, where $\alpha(f) \approx 0.23\alpha(f)$ is the attenuation coefficient in units of km^{-1} . As shown in Appendix B, the transfer function $\mathcal{H}(f)$ is the Fourier transform of the impulse-response function $h(t)$, so that knowledge of one function is sufficient to determine the other.

Three important measures of the performance of the channel are determined from $h(t)$ or $\mathcal{H}(f)$:

- The *attenuation* of a steady (unmodulated) input optical power is determined by the transfer function $\mathcal{H}(f)$ at $f = 0$. Since $\mathcal{H}(f)$ is the Fourier transform of $h(t)$, $\mathcal{H}(0) = \int h(t) dt$ is the area under $h(t)$.
- The *response time* σ_τ is the width of $h(t)$. It limits the shortest time at which adjacent pulses may be spaced without significantly overlapping.
- The *bandwidth* σ_f (Hz) is the width of $|\mathcal{H}(f)|$. It serves as a measure of the maximum rate at which the input power may be modulated without significant increase of the attenuation. Since $\mathcal{H}(f)$ and $h(t)$ are related by a Fourier transform, the bandwidth σ_f is inversely proportional to the response time σ_τ .

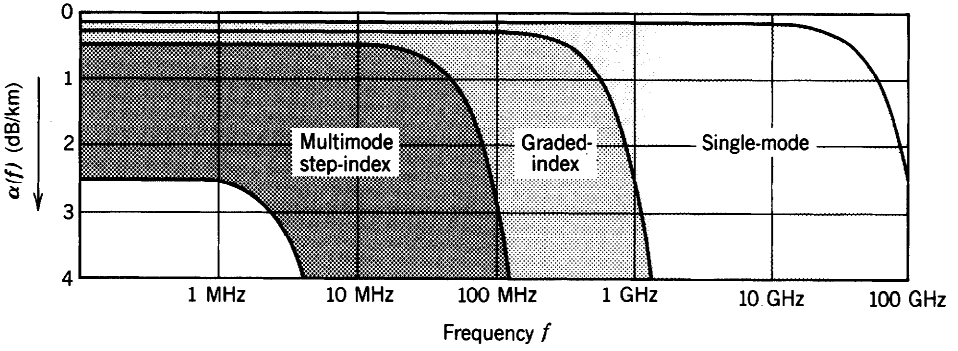


Figure 22.1-4 Typical attenuation coefficients (dB/km) as a function of the modulation frequency f for transmission through different types of optical fibers at various wavelengths. A wave whose power is modulated at frequency f is attenuated by $\alpha(f)L$ dB upon propagation a distance L km. The unmodulated wave is attenuated at a rate $\alpha = \alpha(0)$ dB/km, where α is the attenuation coefficient shown in Fig. 22.1-2.

The coefficient of proportionality depends on the actual profile of $h(t)$ (see Appendix A, Sec. A.2). We use the relation

$$\sigma_f = \frac{1}{2\pi\sigma_\tau}, \quad (22.1-5)$$

Fiber Bandwidth

for purposes of illustration.

The impulse-response function and the transfer function of the optical fiber depend on material attenuation, material and waveguide dispersion, and modal dispersion in the multimode case. The relative contribution of each of these factors depends on the type of fiber: step-index or graded-index, and multimode or single-mode, as illustrated in Fig. 22.1-1 (see also Fig. 8.3-8) and Fig. 22.1-4.

Examples

- In a *multimode step-index fiber* the impulse-response function is a sequence of pulses centered at the mode delay times $\tau_q = L/v_q$, $q = 1, \dots, M$, where v_q is the group velocity of mode q and M is the number of modes (see Fig. 8.3-7). The largest delay difference is $2\sigma_\tau = \tau_{\max} - \tau_{\min}$ where σ_τ is given by (22.1-1). The widths of these pulses are determined by material and waveguide dispersion and are usually much smaller than the delay difference $\tau_{\max} - \tau_{\min}$. A multimode step-index glass fiber with $n_1 = 1.46$ and fractional refractive index difference $\Delta = 0.01$, for example, has a response time $\sigma_\tau/L \approx \Delta/2c_1 \approx 24$ ns/km, corresponding to a bandwidth $\sigma_f L \approx L/2\pi\sigma_\tau \approx 6.5$ MHz-km. For a fiber of length $L = 10$ km, $\sigma_\tau \approx 240$ ns and $\sigma_f \approx 650$ kHz. In a 100-km fiber, an impulse spreads to a width of $2.4 \mu\text{s}$ and the bandwidth drops to 65 kHz.
- The response time of a multimode *graded-index fiber* with an optimal refractive-index profile, $n_1 = 1.46$, and $\Delta = 0.01$ under ideal conditions is, from (22.1-2), $\sigma_\tau/L \approx \Delta^2/4c_1 \approx 122$ ps/km. This corresponds to a bandwidth of 1.3 GHz-km.

Under these conditions, however, material dispersion may become important, depending on the spectral linewidth of the source.

- For a *single-mode fiber* with a light source of spectral linewidth $\sigma_\lambda = 1$ nm (from a typical single-mode laser) and a fiber dispersion coefficient $D_\lambda = 1$ ps/km-nm (for operation near $\lambda_o = 1.3$ μ m), the response time given by (22.1-3) is $\sigma_\tau/L = 1$ ps/km, corresponding to a bandwidth $\sigma_f = 159$ GHz-km. A fiber of length 100 km has a response time 100 ps and bandwidth ≈ 1.6 GHz.

Advanced Materials

Several materials, with attenuation coefficients far smaller than that of silica glass, are being used in experimental optical systems in the mid-infrared region. These include heavy-metal fluoride glasses, halide-containing crystals, and chalcogenide glasses. For these materials, the infrared absorption band is located further in the infrared than in silica glass so that mid-infrared operation, with its attendant reduced Rayleigh scattering (which decreases as $1/\lambda_o^4$), is possible. Attenuations as small as 0.001 dB/km are expected to be achievable with fluoride-glass fibers operating at wavelengths in the 2 to 4 μ m band. If these extremely low-loss materials are economically made into fibers, and if suitable semiconductor light sources are perfected for room-temperature operation in the mid-infrared band, repeaterless transmission over distances of several thousand, instead of hundreds, of kilometers would become routine.

Fiber Amplifiers

Erbium-doped silica fibers, serving as laser amplifiers (see Sec. 13.2C), are becoming increasingly important components of 1.55- μ m fiber-optic communication systems. These devices offer high-gain amplification (30 to 45 dB), with low noise, near the wavelength of lowest loss in silica glass. They are pumped by InGaAsP diode lasers (usually at 1.48 μ m), and exhibit low insertion loss (< 0.5 dB) and polarization insensitivity. They are usually operated in the saturated regime and exhibit minimal crosstalk between different signals that are simultaneously transmitted through them.

An Er^{3+} -doped fiber amplifier may be used as an optical-power amplifier placed directly at the output of the source laser, or as an optical preamplifier at the photodetector input (or both). It can also serve as an all-optical repeater, replacing the electronic repeaters that provide reshaping, retiming, and regeneration of the bits (e.g., those used in current long-haul undersea fiber-optic systems). All-optical repeaters are advantageous in that they offer increased gain and bandwidth, insensitivity to bit rate, and the ability to simultaneously amplify multiple optical channels.

Nonlinear Optical Properties of Fibers

At high levels of power (tens of milliwatts), optical fibers exhibit nonlinear properties, which have a number of undesirable effects such as an increase of the pulse spreading in single-mode fibers, crosstalk between counter-propagating waves used in two-way communications, and crosstalk between waves of different wavelengths used in wavelength-division multiplexing. However, the nonlinear properties of fibers may be harnessed for useful applications. Nonlinear dispersion (dependence of the phase velocity on the intensity) may be adjusted to compensate for chromatic dispersion in the fiber. The result is spreadless pulses known as optical solitons (see Sec. 19.8). The gain provided by a fiber amplifier can be used to compensate for the fiber attenuation so that ideally the pulses suffer no attenuation and no spreading. Nonlinear interactions can also be used to provide gain, but the properties of such amplifiers are generally inferior to those of laser amplifiers such as Er^{3+} :silica fiber.

B. Sources for Optical Transmitters

The basic requirements for the light sources used in optical communication systems depend on the nature of the intended application (long-haul communication, local-area network, etc.). The main features are:

- *Power.* The source power must be sufficiently high so that after transmission through the fiber the received signal is detectable with the required accuracy.
- *Speed.* It must be possible to modulate the source power at the desired rate.
- *Linewidth.* The source must have a narrow spectral linewidth so that the effect of chromatic dispersion in the fiber is minimized.
- *Noise.* The source must be free of random fluctuations. This requirement is particularly strict for coherent communication systems.
- Other features include ruggedness, insensitivity to environmental changes such as temperature, reliability, low cost, and long lifetime.

Both light-emitting diodes (LEDs) and laser diodes are used as sources in fiber-optic communication systems. These devices are discussed in Chap. 16.

Laser diodes have the advantages of high power (tens of mW), high speeds (in the GHz region), and narrow spectral width. However, they are sensitive to temperature variations. Multimode diode lasers suffer from partition noise, i.e., random distribution of the laser power among the modes. When combined with chromatic dispersion in the fiber, this leads to random intensity fluctuations and reshaping of the transmitted pulses. Laser diodes also suffer from frequency chirping, i.e., variation of the laser frequency as the optical power is modulated. Chirping results from changes of the refractive index that accompany changes of the charge-carrier concentrations as the injected current is altered. Significant advances in semiconductor laser technology in recent years have resulted in many improvements and in considerable increase of their reliability and lifetime.

Light-emitting diodes are fabricated in two basic structures: surface emitting and edge emitting. *Surface-emitting diodes* have the advantages of ruggedness, reliability, lower cost, long lifetime, and simplicity of design. However, their basic limitation is their relatively broader linewidth (more than 100 nm in the band 1.3 to 1.6 μm). When operated at their maximum power, modulation frequencies up to 100 Mb/s are possible, but higher speeds (up to 500 Mb/s) can only be achieved at reduced powers. The *edge-emitting diode* has a structure similar to the diode laser (with the reflectors removed). It produces more power output with relatively narrower spectral linewidth, at the expense of complexity.

Sources at 0.87 μm

AlGaAs light-emitting diodes and AlGaAs/GaAs double-heterostructure and quantum-well laser diodes have been used at this wavelength. Surface-emitting LEDs are used extensively.

Sources at 1.3 and 1.55 μm

InGaAsP LEDs have been used in this band with moderate speeds and powers. Single-mode systems make use of InGaAsP/InP double-heterostructure lasers together with single-mode fibers. The requirement for a narrow spectral linewidth is not as crucial at 1.3 μm since material dispersion is minimal. At 1.55 μm , however, it is important to use sources with narrow linewidths because of the presence of material dispersion. A number of technologies are available for providing single-longitudinal-mode lasers (single-frequency lasers) that are stable at high speeds of modulation (see

Sec. 16.3E). These include external-cavity lasers, distributed feedback (DFB) and distributed Bragg-reflector (DBR) lasers capable of providing spectral linewidths of 5 to 100 MHz at a few mW of output power with modulation rates exceeding 20 GHz, and cleaved-coupled-cavity (C^3) lasers which promise linewidths as low as 1 MHz (but are subject to thermal drift).

DFB lasers are probably the most commonly used. Current modulation can be employed since the frequency chirp can be made sufficiently small. DFB lasers with multiple sections and/or multiple electrodes are under development; these should provide further improvements in performance. Quantum-well lasers, in particular InGaAs strained-layer quantum-well lasers (see Sec. 16.3G), are highly promising. These devices offer lower thresholds and larger bandwidths than their lattice-matched cousins (theoretical calculations show that thresholds as low as 50 A/cm², and bandwidths as high as 100 GHz, are possible). The prospects for quantum-wire and quantum-dot lasers (see Sec. 15.1G) lie further in the future.

Sources at Longer Wavelengths

Interest in wavelengths longer than 1.55 μm is engendered by the development of low-loss fibers in the 2- to 4- μm wavelength band. Laser diodes that can be operated at room temperature at these wavelengths are being developed. Double-heterostructure InGaAsSb/AlGaAsSb lasers (lattice matched to a GaSb substrate), as an example, can be operated at $\lambda_o = 2.27 \mu\text{m}$ at $T = 300 \text{ K}$ (so far only in the pulsed mode, however), with a threshold current density $\approx 1500 \text{ A/cm}^2$, differential quantum efficiency ≈ 0.5 , and output power $\approx 2 \text{ W}$. Emission wavelengths from 1.8 to 4.4 μm can potentially be obtained for the range of InGaAsSb compositions that can be lattice matched to GaSb.

C. Detectors for Optical Receivers

A comprehensive discussion of semiconductor photon detectors is provided in Chap. 17. Two types of detectors are commonly used in optical communication systems: the *p-i-n* photodiode and the avalanche photodiode (APD). The APD has the advantage of providing gain before the first electronic amplification stage in the receiver, thereby reducing the detrimental effects of circuit noise. However, the gain mechanism itself introduces noise and has a finite response time, which may reduce the bandwidth of the receiver. Furthermore, APDs require a high-voltage supply and more complicated circuitry to compensate for their sensitivity to temperature fluctuations. The signal-to-noise ratio and the sensitivity of receivers using *p-i-n* photodiodes and APDs are discussed in Secs. 17.5 and 22.4.

Detectors at 0.87 μm

Silicon *p-i-n* photodiodes and APDs are used at these wavelengths. In state-of-the-art preamplifiers, silicon APDs enjoy a 10-to-15-dB sensitivity advantage over silicon *p-i-n* photodiodes because their internal gain makes the noise of the preamplifier relatively less important. The sensitivity of Si APDs at bit rates up to several hundred Mb/s corresponds to about 100 photons/bit. (For a discussion of receiver sensitivity, see Sec. 22.4.)

Detectors at 1.3 and 1.55 μm

Silicon is not usable in this region because its bandgap is greater than the photon energy. Germanium and InGaAs *p-i-n* photodiodes are both used; InGaAs is preferred because it has greater thermal stability and lower dark noise. Typical InGaAs *p-i-n* photodiodes have quantum efficiencies ranging from 0.5 to 0.9, responsivities $\approx 1 \text{ A/W}$, and response times that are in the tens of ps (corresponding to bandwidths up to

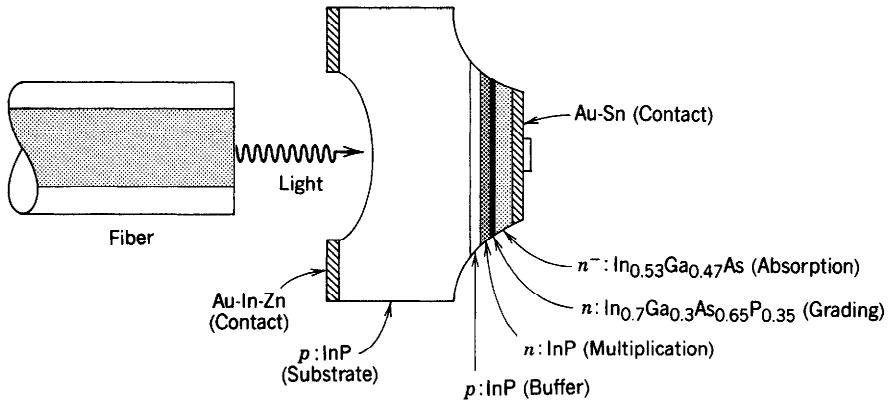


Figure 22.1-5 Structure of an SAGM APD. (Adapted from J. C. Campbell, A. G. Dentai, W. S. Holden, and B. L. Kasper, High-Performance Avalanche Photodiode with Separate Absorption, ‘Grading’, and Multiplication Regions, *Electronics Letters*, vol. 19, pp. 818–820, 1983.)

60 GHz). Some of these devices make use of waveguide structures. Schottky-barrier photodiodes are faster; their response times are in the ps regime, corresponding to bandwidths ≈ 100 GHz.

The development of low-noise APDs (for applications such as fiber-optic communications) has been a challenge. InGaAs APDs operating at speeds ≈ 2 Gb/s are widely available. However since the ionization ratio k is near unity, the gain noise is large. Furthermore, like all narrow bandgap materials, InGaAs suffers from large tunneling leakage currents when subjected to strong electric fields.

A solution to this latter problem makes use of a heterostructure of two materials—a small gap material for the absorption region, and a large-gap material for the multiplication region. Fig. 22.1-5 illustrates an SAGM (separate absorption, grading, multiplication) APD in which the absorption takes place in InGaAs and the multiplication in InP. The InGaAsP grading layer provides a smooth transition for the valence band edge which minimizes hole trapping and shortens the response time of the device. Holes multiply in this device. Quantum efficiencies are in the range 0.75 to 0.9, bandwidths extend up to ≈ 10 GHz, and gain-bandwidth products are as high as ≈ 75 GHz.

At longer wavelengths, junction photodiodes fabricated from II–VI materials (e.g., HgCdTe) and IV–VI materials (e.g., PbSnTe) are useful.

D. Fiber-Optic Systems

The various operating wavelengths and types of fibers, light sources, and detectors that may be used for building an optical link offer many possible combinations, some of which are summarized in Table 22.1-2.

Progress in the implementation of fiber-optic systems has generally followed a downward path along each of the columns of this table, toward longer wavelengths: from multimode to single-mode fibers, from LEDs to lasers, and from photodiodes to APDs. Appropriate materials for the longer wavelengths (e.g., quaternary sources and detectors) had to be developed to make this progress possible. Although there are many possible combinations of the different types of fibers, sources, and detectors, any number of which may be appropriate for certain applications, three systems are particularly noted:

System 1: Multimode Fibers at $0.87\ \mu\text{m}$. This is the early technology of the 1970s. Fibers are either step-index or graded-index. The light source is either an LED or a laser (AlGaAs). Both silicon *p-i-n* and APD photodiodes are used. The

TABLE 22.1-2 Operating Wavelengths and Frequently Used Components in Fiber-Optic Links

Wavelength λ_o (μm)	Fiber	Source		Detector
0.87	Multimode step-index	LED	AlGaAs	Si
1.3	Multimode graded-index			<i>p-i-n</i>
1.55	Single-mode			Ge
		Laser	InGaAsP	APD
				InGaAs

performance of this system is limited by the fiber’s high attenuation and modal dispersion.

System 2: Single-Mode Fibers at 1.3 μm . The move to single-mode fibers and a wavelength where material dispersion is minimal led to a substantial improvement in performance, limited by fiber attenuation. InGaAsP lasers are used with either InGaAs *p-i-n* or APD photodetectors (or Ge APDs).

System 3: Single-Mode Fibers at 1.55 μm . At this wavelength the fiber has its lowest attenuation. Performance is limited by material dispersion, which is reduced by the use of single-frequency lasers (InGaAsP).

These three systems, which are often referred to as the first three generations of fiber-optic systems, are used as examples in Sec. 22.3 and estimates of their expected performance are provided.

Most systems currently being installed belong to the third generation. As an example, the AT&T TAT-9 transatlantic fiber-optic cable (see page 874) makes use of single-mode fibers at 1.55 μm and low-chirp InGaAsP DFB single-frequency lasers. Information is transmitted at 560 Mb/s per fiber pair; some 80,000 simultaneous voice-communication channels are carried the approximately 6000 km from the U.S. and Canada to the U.K., France, and Spain. Repeaters, which are powered by high voltage sent along the length of the cable, are spaced more than 100 km apart.

Third-generation technology has been extended in a number of directions, and systems currently under development will incorporate many of the advances achieved in the laboratory. One relatively recent development of substantial significance is the Er^{3+} :silica-fiber amplifier (see Secs. 13.2C and 22.1A). This device will have a dramatic impact on the configuration of new systems. AT&T and KDD in Japan, for example, have joined together in the development of a transpacific fiber-optic link that will use fiber-amplifier repeaters spaced ≈ 40 km apart to carry some 600,000 simultaneous voice-communication channels. This is a dramatic improvement over the 80,000 simultaneous conversations supported by the electronically repeatered TAT-9 transatlantic cable put into service in 1991.

Optical soliton transmission is another area of high current interest and substantial promise. Solitons are short (typically 1 to 50 ps) optical pulses that can travel through long lengths of optical fiber without changing the shape of their pulse envelope. As discussed in Sec. 19.8, the effects of fiber dispersion and nonlinear self-phase modulation (arising, for example, from the optical Kerr effect) precisely cancel each other, so that the pulses act as if they were traveling through a linear nondispersive medium. Erbium-doped fiber amplifiers can be effectively used in conjunction with soliton transmission to overcome absorption and scattering losses. Prototype systems have already been operated at several Gb/s over fiber lengths in excess of 12,000 km. Soliton transmission at Tb/s rates is in the offing.

All of the systems described above make use of **direct detection**, in which only the signal light illuminates the photodetector. Fourth-generation systems make use of **coherent detection** (see Sec. 22.5), in which a locally generated source of light (the local oscillator) illuminates the photodetector along with the signal. Erbium-doped fiber amplifiers are also useful in conjunction with heterodyne systems. The use of coherent detection in a fiber-optic communication system improves system performance; however, this comes at the expense of increased complexity. As a result, the commercial implementation of coherent systems has lagged behind that of direct-detection systems.

22.2 MODULATION, MULTIPLEXING, AND COUPLING

A communication system (Fig. 22.2.1) is a link between two points in which a physical variable is *modulated* at one point and observed at the other point. In optical communication systems, this variable may be the optical intensity, field amplitude, frequency, phase, or polarization. To transmit more than one message on the same link, the messages may be marked by some physical attribute that identifies them at the receiver. This scheme is called *multiplexing*. A communication network is a link between multiple points. Messages are transmitted between the different points by a system of *couplers* and *switches* that route the messages to the desired locations. Modulation, multiplexing, coupling, and switching are therefore important aspects of communication systems. This section is a brief introduction to modulation, multiplexing, and coupling in fiber-optic communication systems. Photonic switches are considered in Chap. 21.

A. Modulation

Optical communication systems are classified in accordance with the optical variable that is modulated by the message:

Field Modulation. The optical field may serve as a carrier of very high frequency (2×10^{14} Hz at $\lambda_o = 1.5 \mu\text{m}$, for example). The amplitude, phase, or frequency may be modulated, much as the amplitude, phase, or frequency of electromagnetic fields of lower frequencies (such as radio waves) are varied in amplitude modulation (AM), phase modulation (PM), and frequency modulation (FM) systems (Fig. 22.2-2). Because of the extremely high frequency of the optical carrier, a very wide spectral band is available, and large amounts of information can, in principle, be transmitted.

Intensity Modulation. The optical intensity (or power) may be varied in accordance with a modulation rule by means of which the signal is coded (direct proportionality, for example, as illustrated in Fig. 22.2-3). The optical field oscillations at

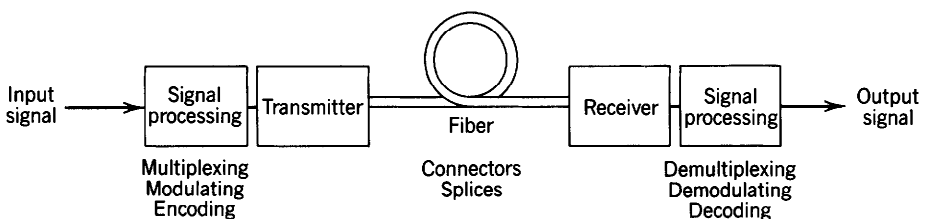


Figure 22.2-1 The fiber-optic communication system.

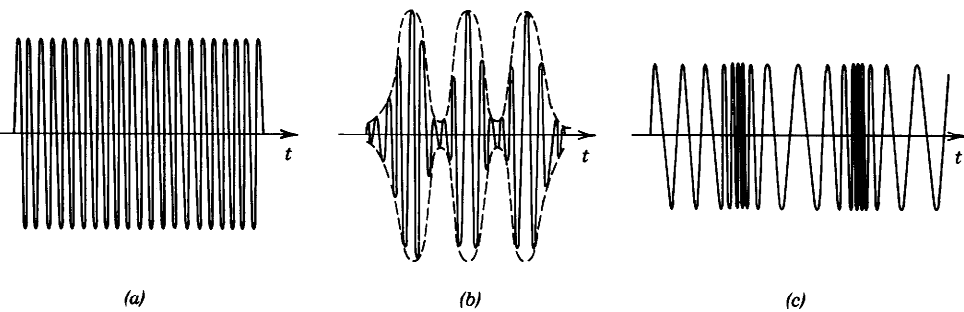


Figure 22.2-2 Amplitude and frequency modulation of the optical field: (a) unmodulated field; (b) amplitude-modulated field; (c) frequency-modulated field.

10^{14} to 10^{16} Hz are unrelated to the operations of modulation and demodulation; only *power* is varied at the transmitter and detected at the receiver. However, the wavelength of light may be used to mark different messages for the purpose of multiplexing.

Although modulation of the optical field is an obvious extension of conventional radio and microwave communication systems to the optical band, it is rather difficult to implement, for several reasons:

- It requires a source whose amplitude, frequency, and phase are stable and free from fluctuations, i.e., a highly coherent laser.
- Direct modulation of the phase or frequency of the laser is usually difficult to implement. An external modulator using the electro-optic effect, for example, may be necessary.
- Because of the assumed high degree of coherence of the source, multimode fibers exhibit large modal noise; a single-mode fiber is therefore necessary.
- Unless a polarization-maintaining fiber is used, a mechanism for monitoring and controlling the polarization is needed.
- The receiver must be capable of measuring the magnitude and phase of the optical field. This is usually accomplished by use of a heterodyne detection system.

Because of the requirement of coherence, optical communication systems using field modulation are called *coherent communication systems*. These systems are discussed in Sec. 22.5.

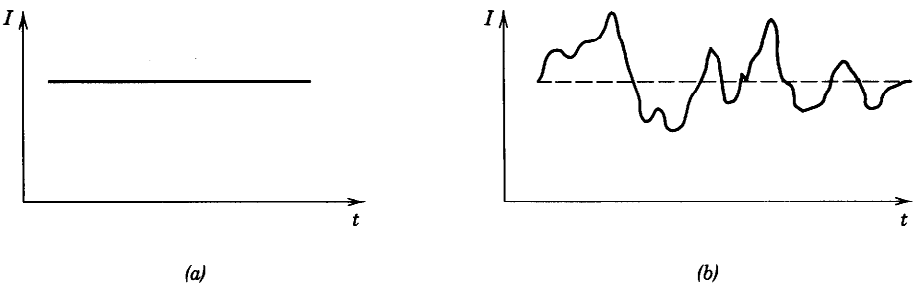


Figure 22.2-3 Intensity modulation: (a) unmodulated intensity; (b) modulated intensity.

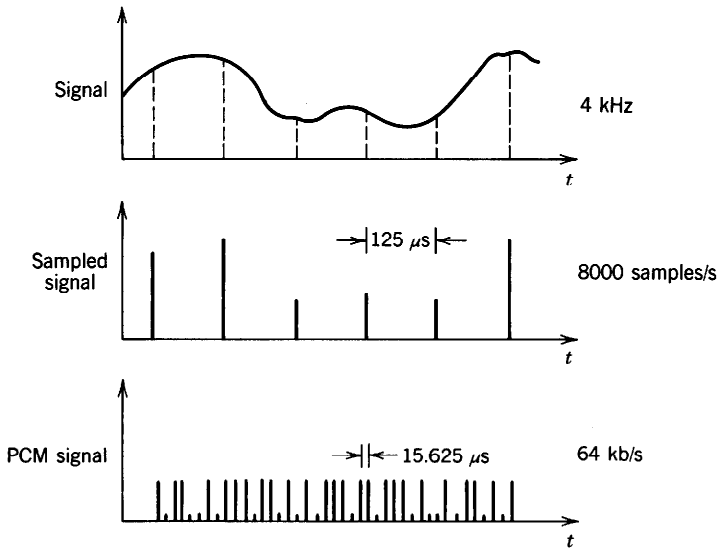


Figure 22.2-4 An example of PCM. A 4-kHz voice signal is sampled at a rate of 8×10^3 samples per second. Each sample is quantized to $2^8 = 256$ levels and represented by 8 bits, so that the signal is a sequence of bits transmitted at a rate of 64 kb/s.

The majority of commercial fiber communication systems at present use intensity modulation. The power of the source is modulated by varying the injected current in an LED or a diode laser. The fiber may be single-mode or multimode and the optical power received is measured by use of a *direct-detection receiver*.

Once the modulation variable is chosen (intensity, frequency, or phase), any of the conventional modulation formats (analog, pulse, or digital) can be used. An important example is **pulse code modulation (PCM)**. In PCM the analog signal is sampled periodically at an appropriate rate and the samples are quantized to a discrete finite number of levels, each of which is binary coded and transmitted in the form of a sequence of binary bits, “1” and “0,” represented by pulses transmitted within the time interval between two adjacent samples (Fig. 22.2-4).

If intensity modulation is adopted, each bit is represented by the presence or absence of a pulse of light. This type of modulation is called **on–off keying (OOK)**. For frequency or phase modulation, the bits are represented by two values of frequency or phase. The modulation is then known as **frequency shift keying (FSK)** or **phase shift keying (PSK)**. These modulation schemes are illustrated in Fig. 22.2-5. It is also possible to modulate the intensity of light with a harmonic function serving as a subcarrier whose amplitude, frequency, or phase is modulated by the signal (in the AM, FM, PM, FSK, or PSK format).

B. Multiplexing

Multiplexing is the transmission and retrieval of more than one signal through the same communication link, as illustrated in Fig. 22.2-6. This is usually accomplished by marking each signal with a physical label that is distinguishable at the receiver. Two standard multiplexing systems are in use: frequency-division multiplexing (FDM) and time-division multiplexing (TDM). In FDM, carriers of distinct frequencies are modulated by the different signals. At the receiver, the signals are identified by the use of filters tuned to the carrier frequencies. In TDM, different interleaved time slots are

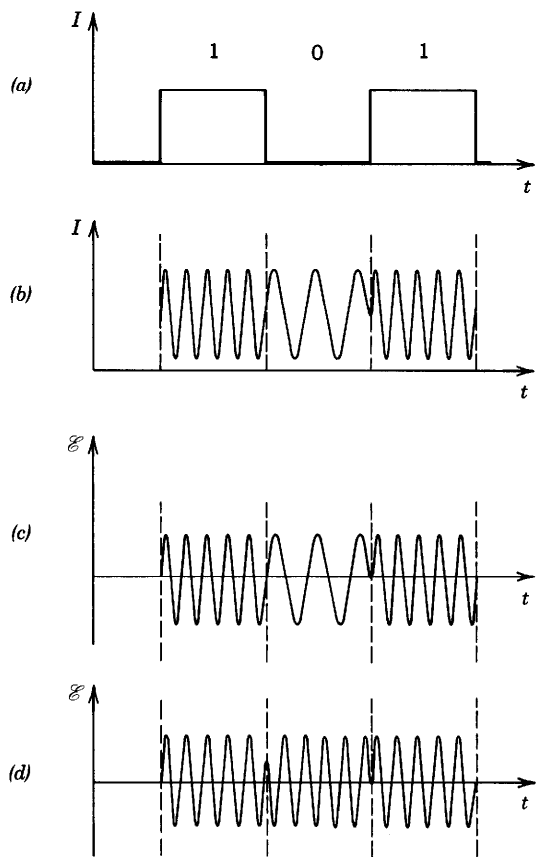


Figure 22.2-5 Examples of binary modulation of light: (a) on-off keying intensity modulation (OOK/IM); (b) frequency-shift-keying intensity modulation (FSK/IM); (c) frequency-shift-keying (FSK) field modulation; (d) phase-shift-keying (PSK) field modulation.

allotted to samples of the different signals. The receiver looks for samples of each signal in the appropriate time slots.

In optical communication systems based on intensity modulation, FDM may be implemented by use of subcarriers of different frequencies. The subcarriers are identified at the receiver by use of electronic filters sensitive to these frequencies, as illustrated in Fig. 22.2-7. It is also possible, and more sensible, to use the underlying optical frequency of light as a multiplexing “label” for FDM. When the frequencies of the carriers are widely spaced (say, greater than a few hundred GHz) this form of FDM is usually called **wavelength-division multiplexing (WDM)**. A WDM system uses light sources of different wavelengths, each intensity modulated by a different signal. The

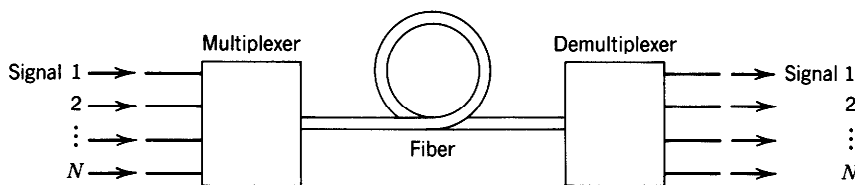


Figure 22.2-6 Transmission of N optical signals through the same fiber by use of multiplexing.

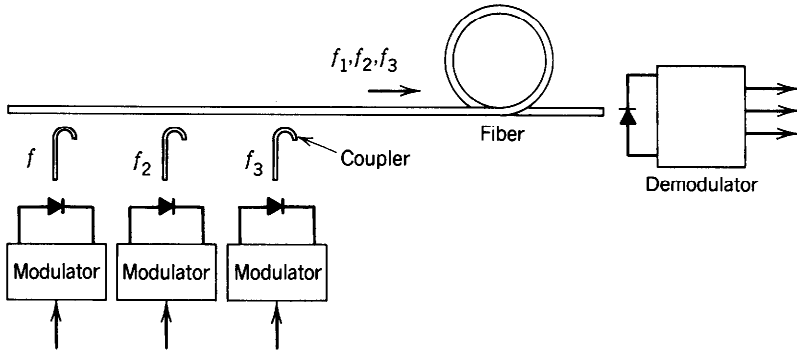


Figure 22.2-7 Frequency-division multiplexing using intensity modulation with subcarriers. Demultiplexing is accomplished by use of electronic filters.

modulated light beams are mixed into the fiber using optical couplers. Demultiplexing is implemented at the receiver end by use of optical (instead of electronic) filters that separate the different wavelengths and direct them to different detectors.

At $\lambda_o = 1.55 \mu\text{m}$, for example, a frequency spacing of $\Delta\nu = 250 \text{ GHz}$ is equivalent to $|\Delta\lambda| = (\lambda_o^2/c_o)|\Delta\nu| = 2 \text{ nm}$. Thus 10 channels cover a band of 20 nm. Since the carrier frequencies are widely spaced, each channel may be modulated at very high rates without crosstalk. However, from an optics perspective, a 2-nm spectral range is relatively narrow. The spectral linewidth of the light sources must be even narrower and their frequencies must be stable within this narrow spectral range.

Wavelength-division demultiplexers use optical filters to separate the different wavelengths. There are filters based on selective absorption, transmission, or reflection, such as thin-film interference filters. An optical fiber, with the two ends acting as reflectors, can serve as a Fabry–Perot etalon with spectral selectivity (see Sec. 2.5B). Other filters are based on angular dispersion, such as the diffraction grating. Examples of these filters are illustrated in Fig. 22.2-8. Another alternative is the use of hetero-

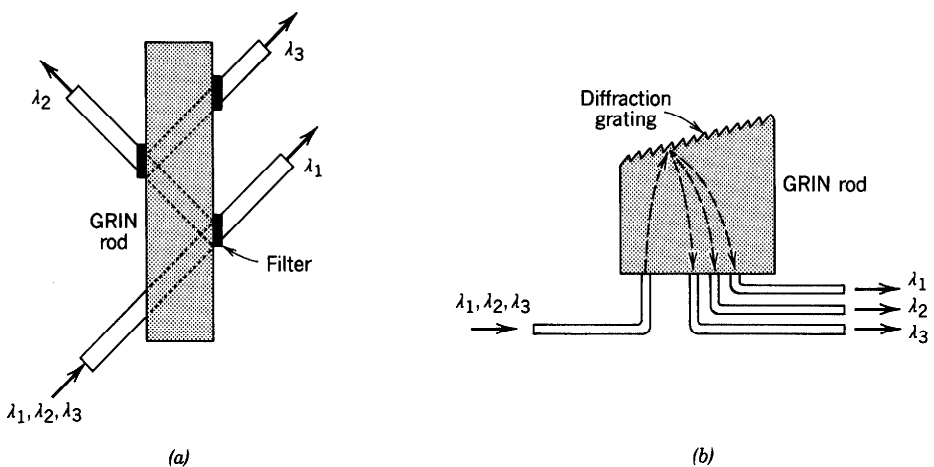


Figure 22.2-8 Wavelength-division demultiplexing using optical filters. (a) Each of the dielectric interference filters transmits only a single wavelength and reflects other wavelengths. A graded-index (GRIN) rod (see Sec. 1.3B) guides the waves between the filters. (b) A diffraction grating (Sec. 2.4B) separates the different wavelengths into different directions, and a graded-index (GRIN) rod guides the waves to the appropriate fibers.

dyne detection. A wavelength-multiplexed optical signal with carrier frequencies ν_1, ν_2, \dots is mixed with a local oscillator of frequency ν_L and detected. The photocurrent carries the signatures of the different carriers at the beat frequencies $f_1 = \nu_1 - \nu_L$, $f_2 = \nu_2 - \nu_L, \dots$. These frequencies are then separated using electronic filters (see Sec. 22.5A).

C. Couplers

In addition to the transmitter, the fiber link, and the receiver, a communication system uses couplers and switches which direct the light beams that represent the various signals to their appropriate destinations. *Couplers* always operate on the incoming signals in the same manner. *Switches* are controllable couplers that can be modified by an external command. Photonic switches are described in Chap. 21.

Examples of couplers are shown schematically in Fig. 22.2-9. In the T-coupler, a signal at input point 1 reaches both output points 2 and 3; a signal at either point 2 or point 3 reaches point 1. In the star coupler, the signal at any of the input points reaches all output points. In the four-port directional coupler, a signal at any of the input points 1 or 2 reaches both output points 3 and 4; and a signal coming from any of the output points 3 or 4 in the opposite direction reaches both points 1 and 2. When operated as a switch, the four-port directional coupler is switched between the parallel state (1–3 and 2–4 connections) and the cross state (1–4 and 2–3 connections).

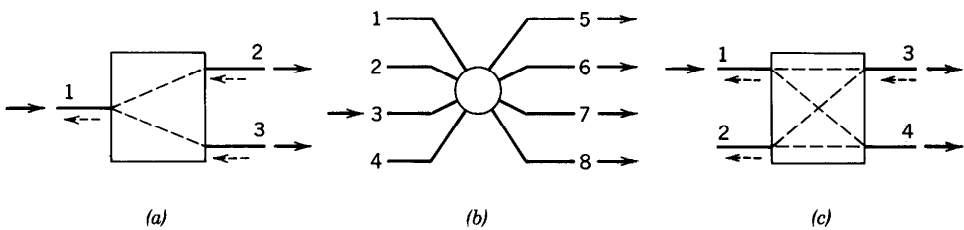


Figure 22.2-9 Examples of couplers: (a) T coupler; (b) star coupler; (c) directional coupler.

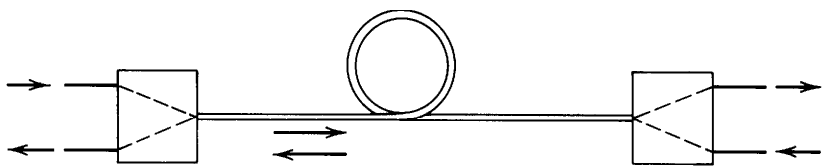


Figure 22.2-10 A duplex (two-way) communication system using two T couplers.

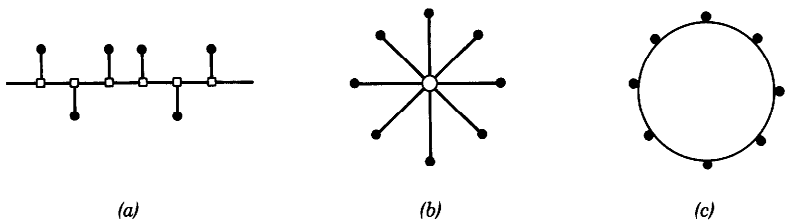


Figure 22.2-11 Examples of communication networks using couplers: (a) bus network; (b) star network; (c) ring network.

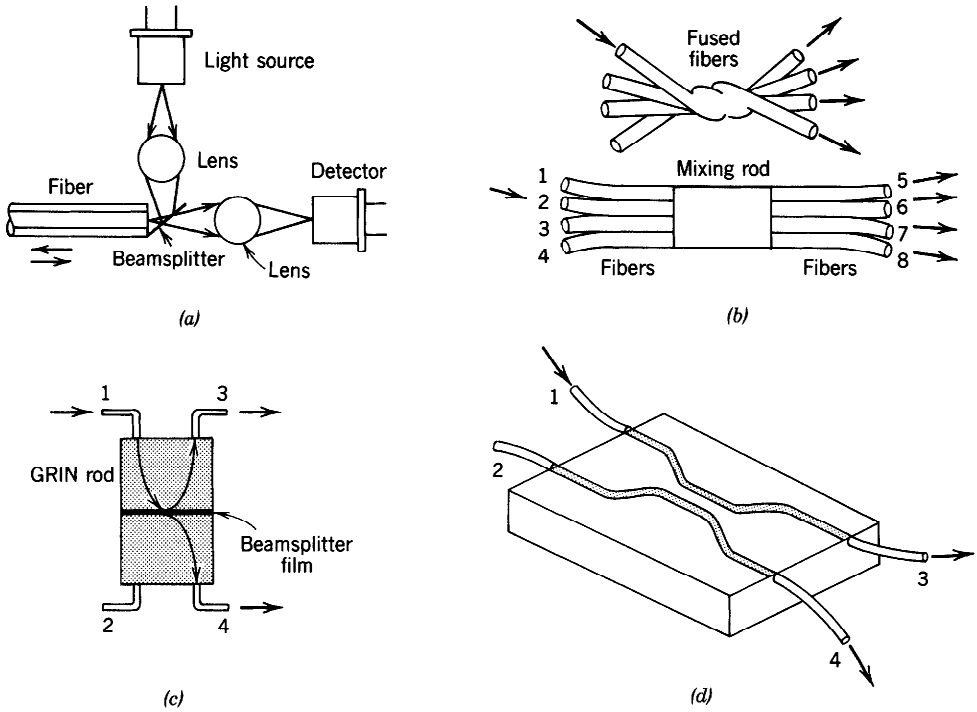


Figure 22.2-12 (a) A T coupler at one end of a duplex optical communication link using a beamsplitter and ball lenses (see Problem 1.2-4). (b) A star coupler using fused fibers and another using a mixing rod, a slab of glass through which light from one fiber is dispersed to reach all other fibers. (c) A four-port directional coupler using two GRIN-rod lenses separated by a beamsplitter film. (d) An integrated-optic four-port directional coupler (see Secs. 7.4B and 21.1B).

An important example illustrating the need for T-couplers is the duplex communication system used in two-way communications, as shown in Fig. 22.2-10. Couplers are essential to communication networks, as illustrated in Fig. 22.2-11. Optical couplers can be constructed by use of miniature beamsplitters, lenses, graded-index rods, prisms, filters, and gratings compatible with the small size of the optical beams transmitted by fibers. This new technology is called **micro-optics**. Integrated-optic devices (see Secs. 7.4B and 21.1B) may also be used as couplers; these are more suitable for single-mode guided light. Figure 22.2-12 shows some examples of optical couplers.

22.3 SYSTEM PERFORMANCE

In this section the basic concepts of design and performance analysis of fiber-optic communication systems are introduced using two examples: an on-off keying digital system and an analog system, both using intensity modulation.

A. Digital Communication System

Consider a fiber-optic communication system using an LED or a laser diode of power P_s (mW) and spectral width σ_λ (nm); an optical fiber of attenuation coefficient α (dB/km), response time σ_τ/L (ns/km), and length L (km); and a *p-i-n* or APD

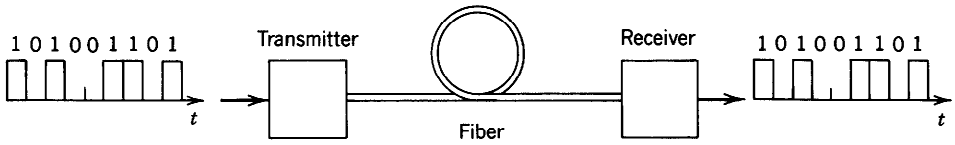


Figure 22.3-1 A binary on-off keying digital optical fiber link.

photodetector. The intensity of light is modulated in an on-off keying (OOK) system by turning the power on and off to represent bits “1” and “0,” as illustrated in Fig. 22.3-1. The link transmits B_0 bits/s. Several of these links may be cascaded to form a longer link. An intermediate receiver-transmitter unit connecting two adjacent links is called a **regenerator** or **repeater**. Here we are concerned only with the design of a single link.

The purpose of the design is to determine the maximum distance L over which the link can transmit B_0 bits/s with a rate of errors smaller than a prescribed rate. Clearly, L decreases with increase of B_0 . An equivalent problem is to determine the maximum bit rate B_0 a link of length L can transmit with an error rate not exceeding the allowable limit. The maximum bit-rate–distance product LB_0 serves as a single number that describes the capability of the link. We shall determine the typical dependence of L on B_0 , and derive expressions for the maximum bit-rate–distance product LB_0 for various types of fibers.

The Bit Error Rate

The performance of a digital communication system is measured by the **probability of error** per bit, which we refer to as the **bit error rate** (BER). If p_1 is the probability of mistaking “1” for “0,” and p_0 is the probability of mistaking “0” for “1,” and if the two bits are equally likely to be transmitted, then $\text{BER} = \frac{1}{2}p_1 + \frac{1}{2}p_0$. A typical acceptable BER is 10^{-9} (i.e., an average of one error every 10^9 bits).

Receiver Sensitivity

The sensitivity of the receiver is defined as the minimum number of photons (or the corresponding optical energy) per bit necessary to guarantee that the rate of error (BER) is smaller than a prescribed rate (usually 10^{-9}). Errors occur because of the randomness of the number of photoelectrons detected during each bit, as well as the noise in the receiver circuit itself. The sensitivity of receivers using different photodetectors will be determined in Sec. 22.4. It will be shown that when the light source is a stabilized laser, the detector has unity quantum efficiency, and the receiver circuit is noise-free, an average of at least $\bar{n}_0 = 10$ photons per bit is required to ensure that $\text{BER} \leq 10^{-9}$. Therefore, *the sensitivity of the ideal receiver is 10 photons/bit*. This means that bit “1” should carry an average of at least 20 photons, since bit “0” carries no photons. In the presence of other forms of noise, the sensitivity may be significantly degraded.

A sensitivity of \bar{n}_0 photons corresponds to an optical energy $h\nu\bar{n}_0$ per bit and an optical power $P_r = (h\nu\bar{n}_0)/(1/B_0)$,

$$P_r = h\nu\bar{n}_0B_0, \quad (22.3-1)$$

which is proportional to the bit rate B_0 . As the bit rate increases, a higher optical power is required to maintain the number of photons/bit (and therefore the BER) constant. It will be shown in Sec. 22.4 that when circuit noise is important, the receiver sensitivity \bar{n}_0 depends on the receiver bandwidth (i.e., on the data rate B_0). This behavior complicates the design problem. For simplicity, we shall assume here that the receiver sensitivity (photons per bit) is independent of B_0 . For the purposes of

illustration we shall use the nominal receiver sensitivities of $\bar{n}_0 = 300$ photons per bit for receivers operating at $\lambda_o = 0.87 \mu\text{m}$ and $1.3 \mu\text{m}$, and $\bar{n}_0 = 1000$ photons per bit for receivers operating at $\lambda_o = 1.55 \mu\text{m}$.

Design Strategy

Once we know the minimum power required at the receiver, the power of the source, and the fiber attenuation per kilometer, a power budget may be prepared from which the maximum fiber length is determined. We must also prepare a budget for the pulse spreading that results from dispersion in the fiber. If the width σ_τ of the received pulses exceeds the bit time interval $1/B_0$, adjacent pulses overlap and cause *intersymbol interference*, which increases the error rates. There are therefore two conditions for the acceptable operation of the link:

- The received power must be at least equal to the receiver power sensitivity P_r . A margin of 6 dB above P_r is usually specified.
- The received pulse width σ_τ must not exceed a prescribed fraction of the bit time interval $1/B_0$.

If the bit rate B_0 is fixed and the link length L is increased, two situations leading to performance degradation may occur: The received power becomes smaller than the receiver power sensitivity P_r , or the received pulses become wider than the bit time $1/B_0$. If the former situation occurs first, the link is said to be *attenuation limited*. If the latter occurs first, the link is said to be *dispersion limited*.

Attenuation-Limited Performance

Attenuation-limited performance is assessed by preparing a power budget. Since fiber attenuation is measured in dB units, it is convenient to also measure power in dB units. Using 1 mW as a reference, dBm units are defined by

$$\mathcal{P} = 10 \log_{10} P, \quad P \text{ in mW; } \mathcal{P} \text{ in dBm.}$$

For example, $P = 0.1 \text{ mW}$, 1 mW , and 10 mW correspond to $\mathcal{P} = -10 \text{ dBm}$, 0 dBm , and 10 dBm , respectively. In these logarithmic units, power losses are additive instead of multiplicative.

If \mathcal{P}_s is the power of the source (dBm), α is the fiber loss in dB/km, \mathcal{P}_c is the splicing and coupling loss (dB), and L is the maximum fiber length such that the power delivered to the receiver is the receiver sensitivity \mathcal{P}_r (dBm), then

$$\mathcal{P}_s - \mathcal{P}_c - \mathcal{P}_m - \alpha L = \mathcal{P}_r \quad (\text{dB units}), \quad (22.3-2)$$

where \mathcal{P}_m is a safety margin. The optical power is plotted schematically in Fig. 22.3-2 as a function of the distance from the transmitter.

The receiver power sensitivity $\mathcal{P}_r = 10 \log_{10} P_r$ (dBm) is obtained from (22.3-1),

$$\mathcal{P}_r = 10 \log \frac{\bar{n}_0 h \nu B_0}{10^{-3}} \text{ dBm.} \quad (22.3-3)$$

Thus \mathcal{P}_r increases logarithmically with B_0 , and the power budget must be adjusted for each B_0 as illustrated in Fig. 22.3-3.

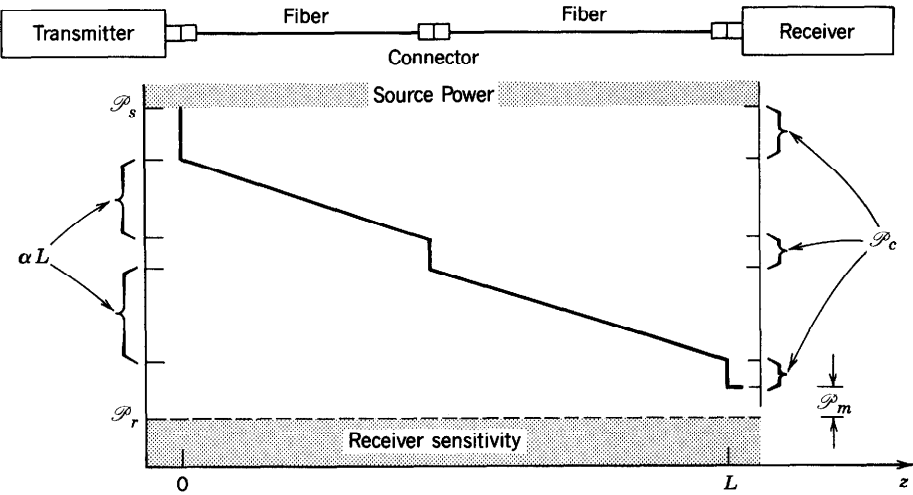


Figure 22.3-2 Power budget of an optical link.

The maximum length of the link is obtained by substituting (22.3-3) into (22.3-2),

$$L = \frac{1}{\alpha} \left(\mathcal{P}_s - \mathcal{P}_c - \mathcal{P}_m - 10 \log \frac{\bar{n}_0 h \nu B_0}{10^{-3}} \right), \tag{22.3-4}$$

from which

$$L = L_0 - \frac{10}{\alpha} \log B_0,$$

(22.3-5)
Distance versus Bit Rate
(Attenuation-Limited Fiber)

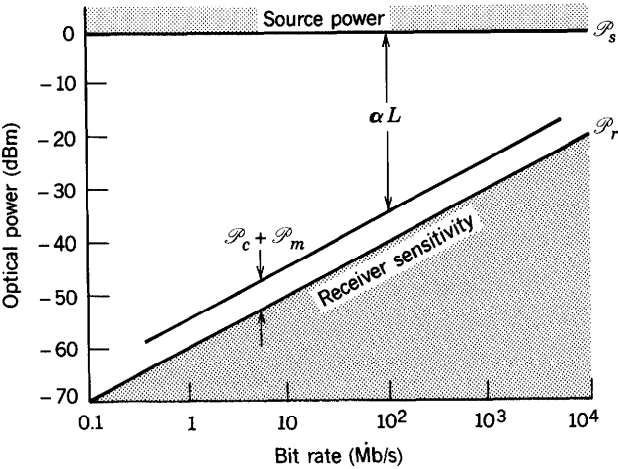


Figure 22.3-3 Power budget as a function of bit rate B_0 . As B_0 increases, the power \mathcal{P}_r required at the receiver increases (so that the energy per bit remains constant), and the maximum length L decreases.

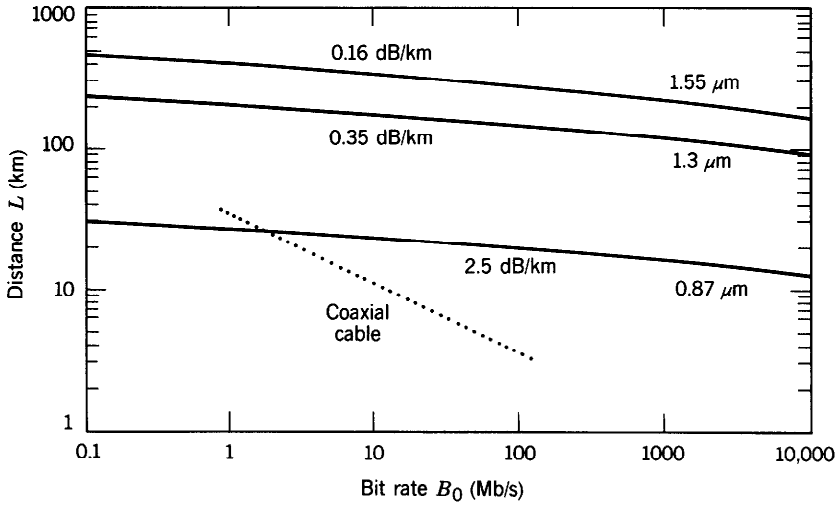


Figure 22.3-4 Maximum fiber length L as a function of bit rate B_0 under attenuation-limited conditions for a fused silica glass fiber operating at wavelengths $\lambda_o = 0.87, 1.3$, and $1.55 \mu\text{m}$ assuming fiber attenuation coefficients $\alpha = 2.5, 0.35$, and 0.16 dB/km , respectively; source power $P_s = 1 \text{ mW}$ ($\mathcal{P}_s = 0 \text{ dBm}$); receiver sensitivity $\bar{n}_0 = 300$ photons/bit for receivers operating at 0.87 and $1.3 \mu\text{m}$ and $\bar{n}_0 = 1000$ for the receiver operating at $1.55 \mu\text{m}$; and $P_c = P_m = 0$. For comparison, the L - B_0 relation for a typical coaxial cable is also shown.

where $L_0 = [\mathcal{P}_s - \mathcal{P}_c - \mathcal{P}_m - 30 - 10 \log(\bar{n}_0 h \nu)] / \alpha$. The length drops with increase of B_0 at a logarithmic rate with slope $10/\alpha$. Figure 22.3-4 is a plot of this relation for the operating wavelengths $0.87, 1.3$, and $1.55 \mu\text{m}$.

Dispersion-Limited Performance

The width σ_τ of the received pulse increases with increase of the fiber length L (see Sec. 22.1A). When σ_τ exceeds the bit time interval, $T = 1/B_0$, the performance begins to deteriorate as a result of intersymbol interference. We shall select the maximum allowed width to be one-fourth of the bit-time interval,

$$\sigma_\tau = \frac{T}{4} = \frac{1}{4B_0}. \quad (22.3-6)$$

The choice of the factor $\frac{1}{4}$ is clearly arbitrary and serves only to compare the different types of fibers:

- **Step-Index Fiber.** The width of the received pulse after propagation a distance L in a multimode step-index fiber is governed by modal dispersion. Substituting (22.1-1) into (22.3-6), we obtain the L - B_0 relation

$$LB_0 = \frac{c_1}{2\Delta}. \quad (22.3-7)$$

Bit-Rate – Distance Product
(Modal-Dispersion-Limited
Step-Index Fiber)

where $c_1 = c_o/n_1$ is the speed of light in the core material and $\Delta = (n_1 - n_2)/n_1$ is the fiber fractional index difference. For $n_1 = 1.46$ and $\Delta = 0.01$, the bit-rate–distance product $LB_0 \approx 10 \text{ km-Mb/s}$.

- **Graded-Index Fiber.** In a multimode graded-index fiber of optimal (approximately parabolic) refractive index profile, the pulse width is given by (22.1-2). Using (22.3-6), we obtain

$$LB_0 = \frac{c_1}{\Delta^2} \quad (22.3-8)$$

Bit-Rate – Distance Product
(Modal-Dispersion-Limited
Graded-Index Fiber)

For $n_1 = 1.46$ and $\Delta = 0.01$, the bit-rate–distance product $LB_0 \approx 2 \text{ km-Gb/s}$.

- **Single-Mode Fiber.** Assuming that pulse broadening in a single-mode fiber results from material dispersion only (i.e., neglecting waveguide dispersion), then for a source of linewidth σ_λ the width of the received pulse is given by (22.1-3), so that

$$LB_0 = \frac{1}{4|D_\lambda|\sigma_\lambda}, \quad (22.3-9)$$

Bit-Rate – Distance Product
(Material-Dispersion-Limited
Single-Mode Fiber)

where D_λ is the dispersion coefficient of the fiber material. For operation near $\lambda_o = 1.3 \mu\text{m}$, $|D_\lambda|$ may be as small as 1 ps/km-nm . Assuming that $\sigma_\lambda = 1 \text{ nm}$ (the linewidth of a single-mode laser), the bit-rate–distance product $LB_0 \approx 250 \text{ km-Gb/s}$. For operation near $\lambda_o = 1.55 \mu\text{m}$, $D_\lambda = 17 \text{ ps/km-nm}$, and for the same source spectral width $\sigma_\lambda = 1 \text{ nm}$, $LB_0 \approx 15 \text{ km-Gb/s}$.

The distance versus bit-rate relations for these dispersion-limited examples are plotted in Fig. 22.3-5.

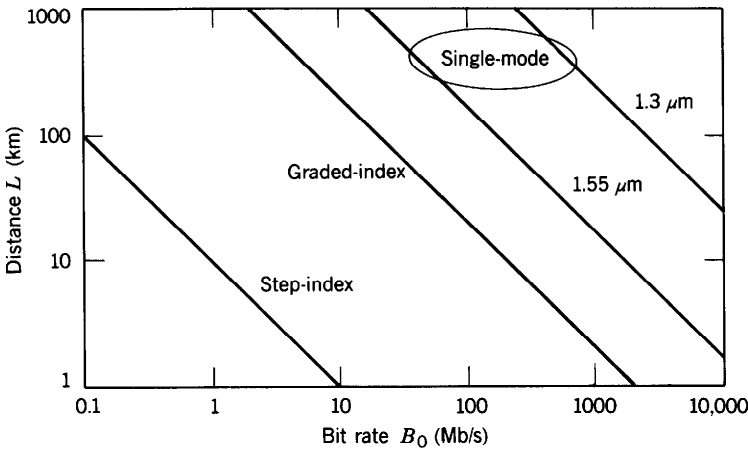


Figure 22.3-5 Dispersion-limited maximum fiber length L as a function of bit rate B_0 for: (a) multimode step-index fiber ($n_1 = 1.46$, $\Delta = 0.01$), $LB_0 = 10 \text{ km-Mb/s}$; (b) multimode graded-index fiber with parabolic profile ($n_1 = 1.46$, $\Delta = 0.01$), $LB_0 = 2 \text{ km-Gb/s}$; (c) single-mode fiber limited by material dispersion, operating at $1.3 \mu\text{m}$ with $|D_\lambda| = 1 \text{ ps/km-nm}$ and $\sigma_\lambda = 1 \text{ nm}$, $LB_0 = 250 \text{ km-Gb/s}$; (d) single-mode fiber limited by material dispersion, operating at $1.55 \mu\text{m}$ with $D_\lambda = 17 \text{ ps/km-nm}$ and $\sigma_\lambda = 1 \text{ nm}$, $LB_0 \approx 15 \text{ km-Gb/s}$.

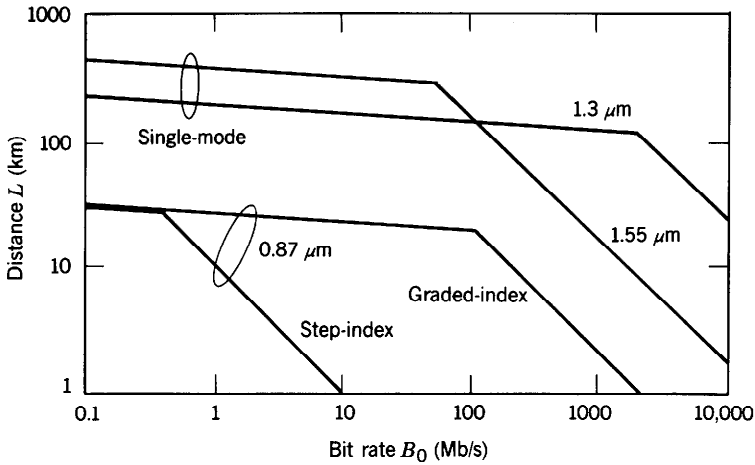


Figure 22.3-6 Maximum distance L versus bit rate B_0 for four examples of fibers. This graph is obtained by superposing the graphs in Figs. 22.3-4 and 22.3-5. Each curve represents the maximum distance L of the link at each bit rate B_0 that satisfies *both* the attenuation and dispersion limits, i.e., guarantees the reception of the required power *and* pulse width at the receiver. At low bit rates, the system is attenuation limited; L drops with B_0 logarithmically. At high bit rates, the system is dispersion limited and L is inversely proportional to B_0 .

The attenuation-limited and dispersion-limited bit-rate–distance relations are combined in Fig. 22.3-6 by superposing Figs. 22.3-4 and 22.3-5. These relations describe the performance of three generations of optical fibers operating at $\lambda_o = 0.87 \mu\text{m}$ (multi-mode step-index and graded-index), at $1.3 \mu\text{m}$ (single-mode), and at $1.55 \mu\text{m}$ (single-mode), respectively.

In creating these L – B_0 curves, many simplifying assumptions and arbitrary choices have been made. The values obtained should therefore be regarded as only indications of the order of magnitude of the relative performance of the different types of fibers.

The Best Possible Fiber-Optic Communication System

It is instructive to compare the performance of the practical systems shown in Fig. 22.3-7 with the “best” that can be achieved with silica glass fibers. The following assumptions are made:

- The fiber is a single-mode fiber operating at $\lambda_o = 1.55 \mu\text{m}$, where the attenuation coefficient is the absolute minimum $\alpha \approx 0.16 \text{ dB/km}$.
- The detector is assumed ideal (i.e., photon limited). This corresponds to a receiver sensitivity of 10 photons per bit, instead of 300 or 1000, which were assumed in the previous examples. Using (22.3-5) the attenuation-limited performance may be determined and is shown in Fig. 22.3-7.
- To reduce the material or waveguide dispersion, the spectral linewidth σ_λ of the source must be small. Spectral widths that are a small fraction of 1 nm are obtained with single-frequency lasers. However, an extremely narrow spectral width is incompatible with an extremely short pulse because of the Fourier transform relation between the spectral and temporal distributions. For a pulse of duration $T = 1/B_0$ the Fourier-transform limited spectral width is[†] $\sigma_\nu \approx 1/2T = B_0/2$. Since $\nu = c_o/\lambda_o$, σ_ν is related to σ_λ by $\sigma_\nu = |\partial\nu/\partial\lambda_o|\sigma_\lambda = (c_o/\lambda_o^2)\sigma_\lambda$. The

[†]This is the power-equivalent spectral width, which is defined by (A.2-10) in Appendix A and satisfies (A.2-12).

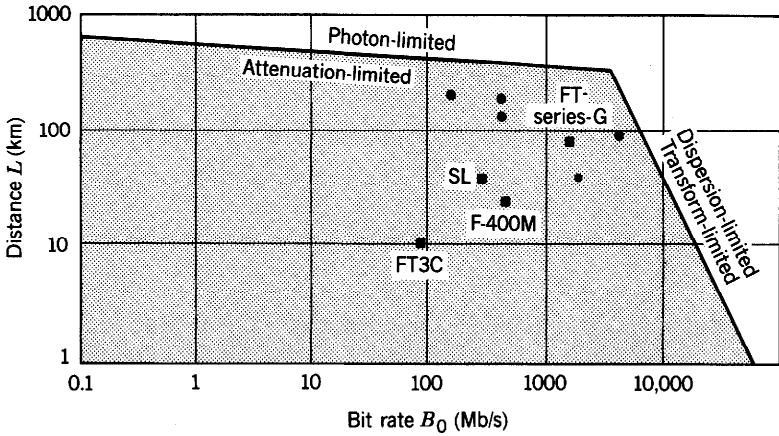


Figure 22.3-7 Distance versus bit rate for a fiber operating at $\lambda_o = 1.55 \mu\text{m}$ with attenuation coefficient $\alpha = 0.16 \text{ dB/km}$ and dispersion coefficient $D_\lambda = 17 \text{ ps/km-nm}$, using an ideal photon-limited receiver with a 10-photon/bit sensitivity and an ideal light source with Fourier-transform-limited spectral width. The squares represent the performance of commercial fiber-optic systems in operation. For example, the AT&T FT-series-G system operates at 1.7 Gb/s with a repeater distance of 90 km at $\lambda_o = 1.55 \mu\text{m}$. The dots represent systems that have been tested in the laboratory. (See, e.g., P. S. Henry, R. A. Linke, and A. H. Gnauck, Introduction to Lightwave Systems, in *Optical Fiber Telecommunications II*, S. E. Miller and I. P. Kaminow, eds., Academic Press, New York, 1988.)

Fourier-transform-limited minimum value of σ_λ is therefore

$$\sigma_\lambda = \frac{\lambda_o^2}{2c_o} B_0, \tag{22.3-10}$$

which is directly proportional to the bit rate B_0 . For $B_0 = 10 \text{ Gb/s}$ and $\lambda_o = 1.55 \mu\text{m}$, for example, $\sigma_\lambda = 0.16 \text{ nm}$. When (22.3-10) is substituted in (22.3-9), we obtain the distance bit-rate relation

$$LB_0^2 = \frac{c_o}{2|D_\lambda|\lambda_o^2}, \tag{22.3-11}$$

which is shown in Fig. 22.3-7 for $\lambda_o = 1.55 \mu\text{m}$ and $D_\lambda = 17 \text{ ps/km-nm}$.

- By use of dispersion-shifted fibers it is possible to reduce the overall chromatic dispersion coefficient D at $1.55 \mu\text{m}$ by a factor of 10, for example. In this case the dispersion-limited line in Fig. 22.3-7 moves to the right to 10 times greater bit rates. However, this comes at the expense of some increase of attenuation, which results in moving the attenuation-limited line downward.

Dispersion as a Power Penalty

The assumption that the maximum acceptable width of the received pulses σ_τ is one-fourth of the bit time $T = 1/B_0$ is rather arbitrary. Wider pulses can in fact be tolerated, provided that the signal-to-noise ratio is improved by increasing the received power beyond the receiver sensitivity. The required increase, denoted \mathcal{P}_{ISI} and called the intersymbol interference power penalty or the **dispersion power penalty**, is deter-

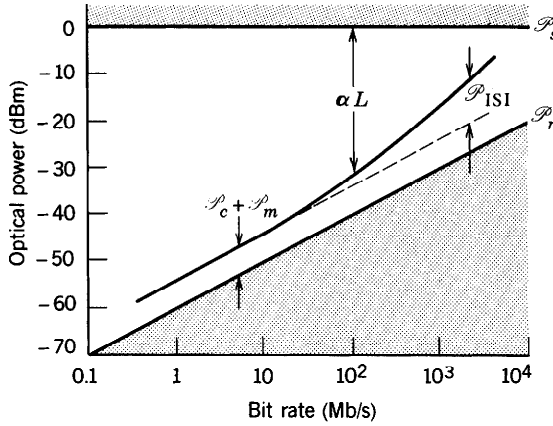


Figure 22.3-8 Power budget as a function of bit rate. \mathcal{P}_s is the source power, \mathcal{P}_c is the power loss at the couplers, \mathcal{P}_r is the receiver sensitivity, \mathcal{P}_m is the power safety margin, and \mathcal{P}_{ISI} is the dispersion power penalty.

mined by ensuring that the error rate reaches the limit $\text{BER} = 10^{-9}$ when the received power is $\mathcal{P}_r + \mathcal{P}_{\text{ISI}}$ and the widths of the received pulses are σ_τ .

A rough estimate of \mathcal{P}_{ISI} may be obtained by determining the attenuation coefficient $\alpha(f)$ [see (22.1-4)] of the fiber at the modulation frequency $f = B_0/2$, which is the frequency of a periodic pulse train representing the bit sequence 101010... The power penalty is then $\mathcal{P}_{\text{ISI}} = [\alpha(f) - \alpha(0)]L$ dB/km. Since σ_τ is the width of the fiber impulse-response function $h(t)$, the width of the transfer function $\mathcal{H}(f)$ is $\sigma_f = 1/2\pi\sigma_\tau$, so that the dispersion-limit condition $\sigma_\tau < 1/4B_0$ is equivalent to $(1/2\pi\sigma_f) < (1/8f)$, or $f < (\pi/4)\sigma_f$. At the prescribed limit $\sigma_\tau = 1/4B_0$, the modulation frequency $f = (\pi/4)\sigma_f$ is well within the fiber bandwidth σ_f so that the penalty is negligible. As σ_τ increases beyond the $1/4B_0$ limit, f eventually exceeds the fiber bandwidth σ_f , whereupon the dispersion power penalty increases sharply. If $h(t)$ is a Gaussian pulse, for example, $\mathcal{H}(f)$ is also Gaussian and its logarithm is proportional to f^2/σ_f^2 , so that the dispersion power penalty in dB units is proportional to $(f/\sigma_f)^2$ or to $(\sigma_\tau/T)^2 = (\sigma_\tau B_0)^2$.

By treating dispersion as a power penalty, the attenuation-limited and dispersion-limited analyses are combined into one general design equation (Fig. 22.3-8)

$$\mathcal{P}_s = \mathcal{P}_c + \mathcal{P}_m + \alpha(f)L + \mathcal{P}_r = \mathcal{P}_c + \mathcal{P}_m + \alpha L + \mathcal{P}_{\text{ISI}} + \mathcal{P}_r. \quad (22.3-12)$$

Since \mathcal{P}_{ISI} is a nonlinear function of B_0 and L , and \mathcal{P}_r is a function of $\log B_0$, (22.3-12) is a nonlinear equation relating L to B_0 . Its solution gives a smooth curve that joins the attenuation-limited and dispersion-limited curves determined earlier in the limits of small and large B_0 , respectively, as illustrated in Fig. 22.3-9.

B. Analog Communication System

An analog fiber-optic communication system using intensity modulation is shown schematically in Fig. 22.3-10. The signal is a continuous function of time representing an audio, video, or data waveform. The power of the light source (usually an LED) is modulated by the signal and guided by the fiber to the receiver, where it is detected and amplified. Under ideal conditions, the original signal is reproduced.

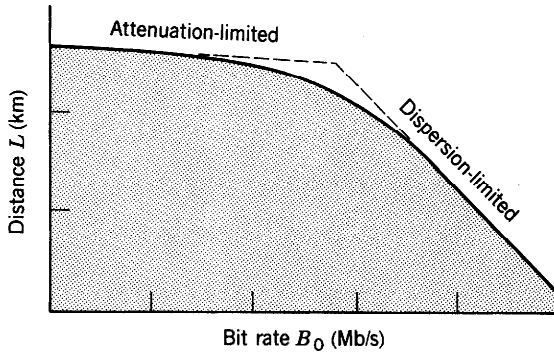


Figure 22.3-9 The L - B_0 relation obtained by treating dispersion as a power penalty.

There are two causes of signal distortion in this type of fiber-optic link:

- Because of the fiber attenuation, the received signal is weakened and may not be discernible from noise.
- Because of the fiber dispersion, the transmission bandwidth is limited and high frequencies are attenuated more than low frequencies, resulting in signal degradation.

Both of these deleterious effects increase with the increase of the fiber length L . The received optical power drops exponentially with L , whereas the fiber bandwidth is inversely proportional to L . The maximum allowable length of the link is determined by ensuring that two conditions are met:

- The fiber attenuation must be sufficiently small so that the received power is greater than the receiver power sensitivity P_r .
- The fiber bandwidth $\sigma_f = 1/2\pi\sigma_\tau$ must be greater than the bandwidth B at which the data are to be transmitted.

As discussed in Sec. 17.5, the sensitivity of an analog optical receiver is the smallest optical power necessary for the signal-to-noise ratio SNR of the photocurrent to exceed a prescribed value SNR_0 . For an ideal receiver (with unity quantum efficiency and no circuit noise) $\text{SNR} = \bar{n} = (P/h\nu)/2B$, where B is the receiver bandwidth, P the optical power (watts), and \bar{n} the average number of photons received in a time interval $1/2B$, regarded as the resolution time of the system. If SNR_0 is the minimum allowed signal-to-noise ratio, the receiver sensitivity becomes $\bar{n}_0 = \text{SNR}_0$ photons per resolution time and the corresponding power

$$P_r = h\nu\bar{n}_0(2B). \quad (22.3-13)$$

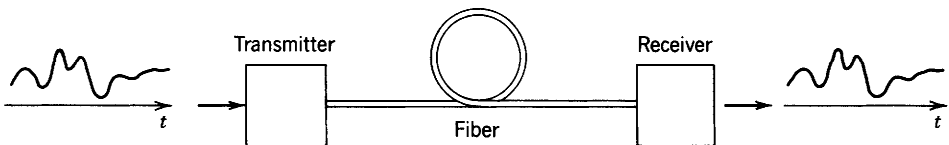


Figure 22.3-10 An analog optical fiber link.

This is identical to the expression (22.3-1) for the power sensitivity of the digital receiver if the resolution time $1/2B$ of the analog system is equated with the bit time $1/B_0$ of the digital system.

Because of the equivalence between (22.3-13) and (22.3-1) and because of the applicability of (22.3-12) to analog systems as well, the $L-B_0$ relations determined earlier for the binary digital system are applicable to the analog system, with B_0 replaced by $2B$, provided that the acceptable performance of the analog system is $\text{SNR}_0 = 10$. As an example, a 1-km fiber link capable of transmitting digital data at a rate of 2 Gb/s with a BER not exceeding 10^{-9} can also be used to transmit analog data of bandwidth 1 GHz with a signal-to-noise ratio of at least 10.

In analog systems, however, the required signal-to-noise ratio is usually much greater than 10, so that the receiver sensitivity must be much greater than 10 photons per resolution time. For high-quality audio and video signals, for example, a 60-dB signal-to-noise ratio is often required. This corresponds to $\text{SNR}_0 = 10^6$, or $\bar{n}_0 = 10^6$ photons per resolution time. Additional design considerations are particularly important in analog systems. For example, the nonlinear response of the light source and photodetector cause additional signal degradation and place restrictions on the dynamic range of the transmitted waveforms.

22.4 RECEIVER SENSITIVITY

The sensitivity of an analog receiver was defined in Sec. 17.5 as the minimum power of the received light (or the corresponding photon flux) necessary to achieve a prescribed signal-to-noise ratio SNR_0 . In this section we discuss the sensitivity of the digital communication receiver. The sensitivity of a binary on-off keying system is defined as the minimum optical energy (or the corresponding mean number of photons) per bit necessary to obtain a prescribed bit error rate (BER). We first determine the sensitivity of the ideal detector and then consider the effects of circuit noise and detector gain noise. This section relies on the material in Sec. 17.5.

Sensitivity of the Ideal Optical Receiver

Assume that bits "1" and "0" of the on-off keying system described in Secs. 22.2A and 22.3A are represented by the presence and absence of optical energy, respectively (Fig. 22.4-1). During bit "1" an average of \bar{n} photons is received. During bit "0" no photons are received. If the two bits are equally likely, the overall average number of photons per bit is $\bar{n}_a = \frac{1}{2}\bar{n}$. Since the actual number of detected photons is random, errors in bit identification occur.

For light generated by laser diodes, the probability of detecting n photons when an average of \bar{n} photons is transmitted obeys the Poisson distribution $p(n) = \bar{n}^n \exp(-\bar{n})/n!$ (see Sec. 11.2). The receiver decides that "1" has been transmitted if it detects one or more photons. The probability p_1 of mistaking "1" for "0" is therefore equal to the probability of detecting no photons, i.e., $p_1 = p(0) = \exp(-\bar{n})$. When bit "0" is transmitted, there are no photons; the receiver decides correctly that bit "0" has been transmitted, so that $p_0 = 0$. The bit error rate is the average of the two error probabilities, $\text{BER} = \frac{1}{2}(p_1 + p_0)$, from which

$$\text{BER} = \frac{1}{2} \exp(-\bar{n}) = \frac{1}{2} \exp(-2\bar{n}_a). \quad (22.4-1)$$

Figure 22.4-1 is a semilogarithmic plot of this relation.

The receiver sensitivity is defined as the average number of photons per bit required to achieve a certain BER (usually 10^{-9}). For $\text{BER} = 10^{-9}$, (22.4-1) gives $\bar{n}_a \approx 10$

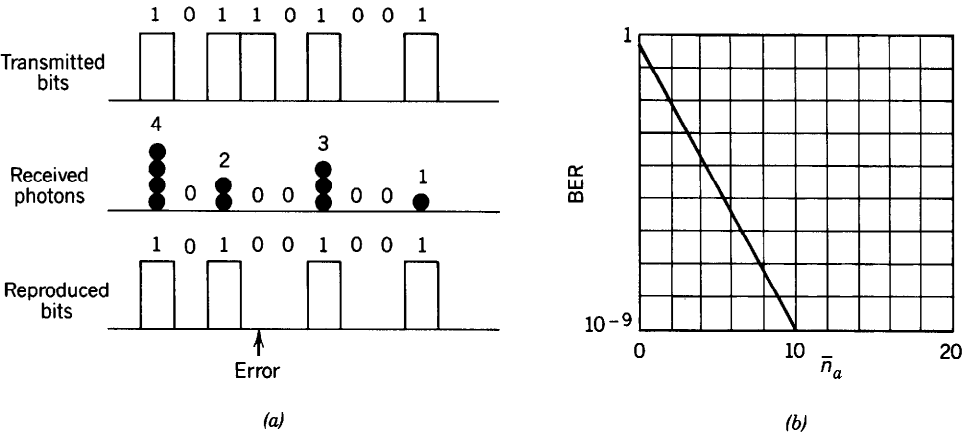


Figure 22.4-1 (a) Example of errors resulting from the random photon numbers. (b) Bit error rate BER versus the mean number of photons per bit \bar{n}_a in an on-off keying system using an ideal receiver.

photons per bit. We conclude that:

The receiver sensitivity (for bit error rate $\text{BER} = 10^{-9}$) of an optical digital communication system using an ideal receiver is 10 photons per bit.

EXERCISE 22.4-1

Effect of Quantum Efficiency and Background Noise on Receiver Sensitivity

- (a) Show that for a receiver using a detector with quantum efficiency η , but otherwise ideal, $\text{BER} = \frac{1}{2} \exp(-2\eta\bar{n}_a)$, and that the sensitivity is $\bar{n}_a = 10/\eta$ photons per bit, corresponding to $\bar{m}_a = \eta\bar{n}_a = 10$ photoelectrons per bit.
- (b) Assuming that bits “1” and “0” correspond to mean photon numbers $\bar{n}_1 = \bar{n} + \bar{n}_B$ and $\bar{n}_0 = \bar{n}_B$, where \bar{n} is the mean number of signal photons and \bar{n}_B is the mean of a Poisson-distributed background photon flux that is always present independently of the signal, determine an expression for the BER as a function of \bar{n} and \bar{n}_B . Plot BER versus $\bar{n}_a = \frac{1}{2}\bar{n}$ for several values of \bar{n}_B . From this plot, determine the receiver sensitivity \bar{n}_a as a function of \bar{n}_B . (Hint: The sum of two random numbers, each with a Poisson probability distribution, also has a Poisson distribution.)

It should be recognized that the ideal receiver sensitivity of 10 photons per bit is applicable only for light with a Poisson photon-number distribution. The sensitivity can, in principle, be improved by the use of photon-number-squeezed light (see Sec. 11.3B).

Sensitivity of a Receiver with Circuit Noise and Gain Noise

As explained in Sec. 17.5, a photodiode transforms an average fraction η of the received photons into photoelectron-hole pairs, each of which contributes a charge e to the electric current in the external circuit. The total charge accumulated in the bit time $T = 1/B_0$ is m (units of electrons). This number is random and has a Poisson distribution with mean $\bar{m} = \eta\bar{n}$ and variance \bar{m} .

Additional noise is introduced by the photodiode circuit in the form of a random electric current i_r of Gaussian probability distribution with zero mean and variance σ_r^2 . Within the bit time interval $T = 1/B_0$, the accumulated charge $q = i_r T/e$ (in units of electrons) has an rms value $\sigma_q = \sigma_r T/e$. The parameter σ_q , called the circuit-noise parameter, depends on the receiver bandwidth B as described in Sec. 17.5C.

The total accumulated charge per bit $s = m + q$ (units of electrons) is the sum of a Poisson random variable m and an independent Gaussian random variable q . Its mean is

$$\mu = \bar{m} = \eta \bar{n} \quad (22.4-2)$$

and its variance is the sum of the variances,

$$\sigma^2 = \bar{m} + \sigma_q^2. \quad (22.4-3)$$

When \bar{m} is large, the overall distribution may be approximated by a Gaussian distribution with mean μ and variance σ^2 . We adopt this approximation in the present analysis.

For an avalanche photodiode (APD) of gain \bar{G} , the mean number of photoelectrons is amplified by a factor \bar{G} , but additional noise is introduced in the amplification process. The mean of the total collected charge per bit s (units of electrons) is

$$\mu = \bar{m}\bar{G} \quad (22.4-4)$$

and the variance is

$$\sigma^2 = \bar{m}\bar{G}^2 F + \sigma_q^2, \quad (22.4-5)$$

where $F = \langle G^2 \rangle / \langle G \rangle^2$ is the excess-noise factor of the APD (see Sec. 17.5B).

The receiver measures the charge s accumulated in each bit (by use of an integrator, for example) and compares it to a prescribed threshold ϑ . If $s > \vartheta$, bit “1” is selected; otherwise, bit “0” is selected. The probabilities of error p_1 and p_0 are determined by examining two Gaussian probability distributions of s that have

$$\begin{aligned} \text{mean } \mu_0 &= 0, & \text{variance } \sigma_0^2 &= \sigma_q^2 & \text{for bit “0”} \\ \text{mean } \mu_1 &= \bar{m}\bar{G}, & \text{variance } \sigma_1^2 &= \bar{m}\bar{G}^2 F + \sigma_q^2 & \text{for bit “1.”} \end{aligned} \quad (22.4-6)$$

The probability p_0 of mistaking “0” for “1” is the integral of a Gaussian probability distribution $p(s)$ with mean μ_0 and variance σ_0^2 from $s = \vartheta$ to $s = \infty$. The probability p_1 of mistaking “1” for “0” is the integral of a Gaussian probability distribution with mean μ_1 and variance σ_1^2 from $s = -\infty$ to $s = \vartheta$. The threshold ϑ is selected such that the average probability of error $\text{BER} = \frac{1}{2}(p_0 + p_1)$ is minimized.

This type of analysis is the basis of the conventional theory of binary detection in the presence of Gaussian noise. If μ_0 and μ_1 , and σ_0^2 and σ_1^2 are the means and variances associated with two Gaussian variables representing bits “0” and “1,” and if σ_0 and σ_1 are much smaller than $\mu_1 - \mu_0$, the bit error rate for an optimal-threshold receiver is approximately

$$\text{BER} \approx \frac{1}{2} \left[1 - \text{erf} \left(\frac{Q}{\sqrt{2}} \right) \right], \quad (22.4-7)$$

where

$$Q = \frac{\mu_1 - \mu_0}{\sigma_0 + \sigma_1} \tag{22.4-8}$$

and

$$\text{erf}(z) = \frac{2}{\sqrt{\pi}} \int_0^z \exp(-x^2) dx \tag{22.4-9}$$

is the error function. When $Q = 6$, $\text{BER} \approx 10^{-9}$. The receiver sensitivity therefore corresponds to $Q = 6$, or

$$\mu_1 - \mu_0 = 6(\sigma_0 + \sigma_1).$$

(22.4-10)

Condition for $\text{BER} = 10^{-9}$
(Gaussian Approximation)

Substituting from (22.4-6) into (22.4-10) and defining $\bar{m}_a = \frac{1}{2}\bar{m}$ as the mean number of photoelectrons detected per bit, we obtain

$$\bar{m}_a = 18F + 6\frac{\sigma_q}{\bar{G}}. \tag{22.4-11}$$

Equation (22.4-11) relates the receiver sensitivity \bar{m}_a , which is the mean number of photoelectrons per bit required to make the $\text{BER} = 10^{-9}$, to the receiver parameters \bar{G} , F , and σ_q .

When the APD gain is sufficiently large so that $3\bar{G}F \gg \sigma_q$, the second term in (22.4-11) is negligible and

$$\bar{m}_a \approx 18F.$$

(22.4-12)

APD Receiver Sensitivity
(No Circuit Noise)

For a receiver using a photodiode with no gain ($\bar{G} = 1$ and $F = 1$) and assuming that the circuit noise is negligible, $\bar{m}_a = 18$ photoelectrons per bit. This is different from the 10 photoelectrons per bit obtained earlier for this ideal receiver. The reason for the discrepancy is that the replacement of the Poisson distribution with the Gaussian distribution is not appropriate in this case. Typical sensitivities of several receivers are listed in Table 22.4-1. The actual values depend on the receiver circuit-noise parameter σ_q , which in turn depends on the bit rate B_0 .

TABLE 22.4-1 Typical Sensitivities (Mean Number of Photons per Bit) of Some Optical Receivers Operating at Bit Rates in the Range 1 Mb/s to 2.5 Gb/s

Receiver	Receiver Sensitivity (photons/bit)
Photon-limited ideal detector	10
Si APD	125
Er-doped silica-fiber preamplifier/ InGaAs <i>p-i-n</i> photodiode	215
InGaAs APD	500
<i>p-i-n</i> photodiode	6000

22.5 COHERENT OPTICAL COMMUNICATIONS

Coherent optical communication systems may use field modulation (amplitude, phase, or frequency) instead of intensity modulation. They employ highly coherent light sources, single-mode fibers, and heterodyne receivers. In this section we examine the principles of operation of these systems, determine their performance advantage, and briefly discuss the requirements on the system components.

A. Heterodyne Detection

Photodetectors are responsive to the photon flux and, as such, are insensitive to the optical phase. It is possible, however, to measure the complex amplitude (both magnitude and phase) of the signal optical field by mixing it with a coherent reference optical field of stable phase, called the **local oscillator**, and detecting the superposition using a photodetector, as illustrated in Fig. 22.5-1. As a result of interference (beating) between the two fields, the detected electric current contains information about both the amplitude and phase of the signal field.

This detection technique is called **optical heterodyning**, **optical mixing**, **photomixing**, **light beating** (see Sec. 2.6B), or **coherent optical detection** (as opposed to **direct detection**). The coherent optical receiver is the optical equivalent of a superheterodyne radio receiver. The signal and local-oscillator waves usually have different frequencies (ν_s and ν_L). When $\nu_s = \nu_L$ the detector is said to be a **homodyne detector**.

Let $\mathcal{E}_s = \text{Re}\{A_s \exp(j2\pi\nu_s t)\}$ be the signal optical field, with $A_s = |A_s| \exp(j\varphi_s)$ its complex amplitude and ν_s its frequency. The magnitude $|A_s|$ or the phase φ_s are modulated with the information signal at a rate much slower than ν_s . The local oscillator field is described similarly by \mathcal{E}_L , A_L , ν_L , and φ_L . The two fields are mixed using a beamsplitter or an optical coupler, as illustrated in Fig. 22.5-1. If the incident fields are perfectly parallel plane waves and have precisely the same polarization, the total field is the sum of the two constituent fields $\mathcal{E} = \mathcal{E}_s + \mathcal{E}_L$. Taking the absolute square of the sum of the complex amplitudes, we obtain

$$\begin{aligned} & |A_s \exp(j2\pi\nu_s t) + A_L \exp(j2\pi\nu_L t)|^2 \\ &= |A_s|^2 + |A_L|^2 + 2|A_s||A_L|\cos[2\pi(\nu_s - \nu_L)t + (\varphi_s - \varphi_L)]. \end{aligned}$$

Since the intensities I_s , I_L , and I are proportional to the absolute-square values of the

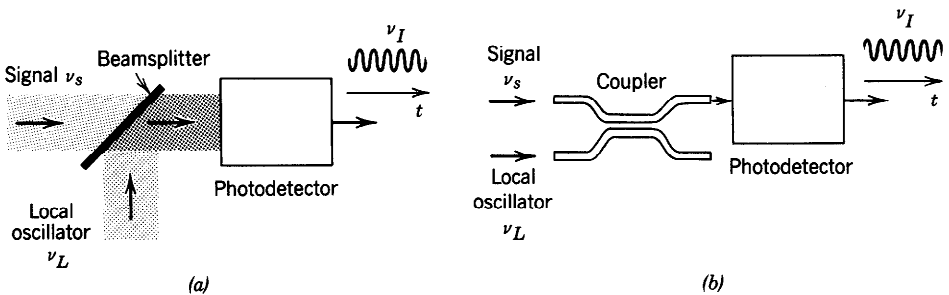


Figure 22.5-1 Optical heterodyne detection. A signal wave of frequency ν_s is mixed with a local oscillator wave of frequency ν_L using (a) a beamsplitter, and (b) an optical coupler. The photocurrent varies at the frequency difference $\nu_I = \nu_s - \nu_L$.

complex amplitudes,

$$I = I_s + I_L + 2(I_s I_L)^{1/2} \cos[2\pi\nu_I t + (\varphi_s - \varphi_L)],$$

where $\nu_I = \nu_s - \nu_L$ is the difference frequency.

The optical power collected by the detector is the product of the intensity and the detector area, so that

$$P = P_s + P_L + 2(P_s P_L)^{1/2} \cos[2\pi\nu_I t + (\varphi_s - \varphi_L)], \quad (22.5-1)$$

where P_s and P_L are the powers of the signal and the local-oscillator beams, respectively. Slight misalignments between the directions of the two waves reduces or washes out the interference term [the third term of (22.5-1)], since the phase $\varphi_s - \varphi_L$ then varies sinusoidally with position within the area of the detector. The third term of (22.5-1) varies with time at the difference frequency ν_I with a phase $\varphi_s - \varphi_L$. If the signal and local oscillator beams are close in frequency, their difference ν_I can be far smaller than the individual frequencies.

The photocurrent i generated in a semiconductor photon detector is proportional to the incident photon flux Φ (see Sec. 17.1B). When ν_I is much smaller than ν_s and ν_L , the superposed light is quasi-monochromatic and the total photon flux $\Phi \approx P/h\bar{\nu}$ is proportional to the optical power, where $\bar{\nu} = \frac{1}{2}(\nu_s + \nu_L)$. The mean photocurrent is therefore $\bar{i} = \eta e \Phi = (\eta e/h\bar{\nu})P$, where e is the electron charge and η the detector's quantum efficiency, so that

$$\bar{i} = \bar{i}_s + \bar{i}_L + 2(\bar{i}_s \bar{i}_L)^{1/2} \cos[2\pi\nu_I t + (\varphi_s - \varphi_L)], \quad (22.5-2)$$

where $\bar{i}_s = \eta e P_s/h\bar{\nu}$ and $\bar{i}_L = \eta e P_L/h\bar{\nu}$ are the photocurrents generated by the signal and local-oscillator individually. The local oscillator is usually much stronger than the signal, so that the first term in (22.5-2) is negligible and

$$\bar{i} \approx \bar{i}_L + 2(\bar{i}_s \bar{i}_L)^{1/2} \cos[2\pi\nu_I t + (\varphi_s - \varphi_L)]. \quad (22.5-3)$$

Photomixing Current

The time dependence of the detected current \bar{i} is sketched in Fig. 22.5-2(a). The second term in (22.5-3), which oscillates at the difference frequency ν_I , carries the

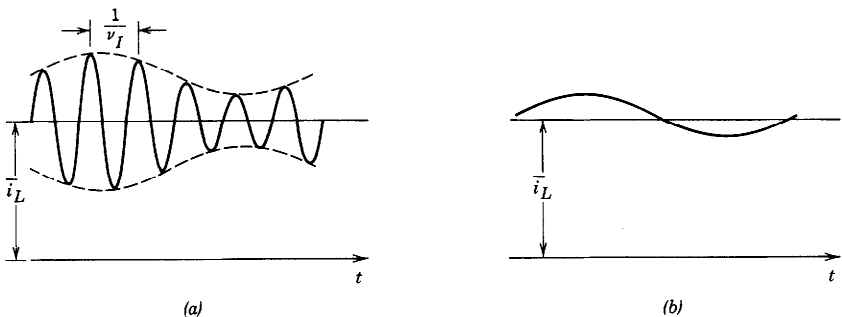


Figure 22.5-2 (a) Photocurrent generated by the heterodyne detector. The envelope and phase of the time-varying component carries complete information about the complex amplitude of the optical field representing the signal. (b) Photocurrent generated by the homodyne detector.

useful information. With knowledge of \bar{i}_L and φ_L , the amplitude and phase of this term can be determined, and \bar{i}_s and φ_s estimated, from which the intensity and phase (and hence the complex amplitude) of the measured optical signal can be inferred. The information-containing signal variables \bar{i}_s or φ_s are usually slowly varying functions of time in comparison with the difference frequency ν_I , so they act as slow modulations of the amplitude and the phase of the harmonic function $2\bar{i}_L^{1/2} \cos(2\pi\nu_I t - \varphi_L)$. This amplitude- and phase-modulated current can be demodulated by drawing on the conventional techniques used in AM and FM radio receivers.

From a photon-optics point of view, this process can be understood in terms of the detection of polychromatic (two-frequency) photons (see Problem 11.1-7).

The homodyne system is a special case of the heterodyne system for which $\nu_s = \nu_L$ and $\nu_I = 0$. The demodulation process is different. A phase-locked loop is used to lock the phase of the local oscillator so that $\varphi_L = 0$ and (22.5-3) yields

$$\bar{i} = \bar{i}_L + 2(\bar{i}_s \bar{i}_L)^{1/2} \cos \varphi_s. \quad (22.5-4)$$

Amplitude and phase modulation is achieved by varying \bar{i}_s or φ_s , respectively.

B. Performance of the Analog Heterodyne Receiver

Heterodyne detection is necessary whenever the phase of the optical field is to be measured. However, heterodyne detection can also be useful for measuring the optical intensity since it provides gain through the presence of the strong local oscillator. As such, it offers an alternative to both laser amplification (see Chap. 13 and Sec. 16.2) and APD amplification (see Sec. 17.4). This can provide a signal-to-noise ratio advantage over direct detection, as we show in this section.

The mean photocurrent \bar{i} generated by a photodiode is accompanied by noise of variance

$$\sigma_i^2 = 2e\bar{i}B + \sigma_r^2, \quad (22.5-5)$$

where B is the receiver's bandwidth; the first term is due to photon noise and the second represents circuit noise (see Sec. 17.5). The intensity of the local oscillator can be made sufficiently large so that even if the signal is weak, the total current \bar{i} is such that the circuit noise σ_r^2 is negligible in comparison with the photon noise $2e\bar{i}B$.

Assuming that $\bar{i}_L \gg \bar{i}_s$ and $2e\bar{i}_L B \gg \sigma_r^2$, we use (22.5-3) and approximate (22.5-5) by

$$\bar{i} \approx \bar{i}_L + 2(\bar{i}_s \bar{i}_L)^{1/2} \cos[2\pi\nu_I t + (\varphi_s - \varphi_L)] \quad (22.5-6a)$$

$$\sigma_i^2 \approx 2e\bar{i}_L B. \quad (22.5-6b)$$

In the case of amplitude modulation, the signal is represented by the rms value of the sinusoidal waveform in (22.5-6a), with the phase ignored. The electrical signal power is therefore $\frac{1}{2}[2(\bar{i}_s \bar{i}_L)^{1/2}]^2 = 2\bar{i}_s \bar{i}_L$ and the noise power is $\sigma_i^2 = 2e\bar{i}_L B$, so that the power signal-to-noise ratio is

$$\text{SNR} = \frac{2\bar{i}_s \bar{i}_L}{2e\bar{i}_L B} = \frac{\bar{i}_s}{eB}. \quad (22.5-7)$$

If $\bar{m} = \bar{i}/2Be$ is the mean number of photoelectrons counted in the resolution time

interval $T = 1/2B$, then

$$\boxed{\text{SNR} = 2\bar{m}}. \quad (22.5-8)$$

Signal-to-Noise Ratio
of a Heterodyne Receiver

In comparison, the SNR of the direct-detection photodiode receiver measuring the same signal current \bar{i}_s without the benefit of heterodyning is

$$\text{SNR} = \frac{\bar{i}_s^2}{2e\bar{i}_sB + \sigma_r^2} = \frac{\bar{m}^2}{\bar{m} + \sigma_q^2}, \quad (22.5-9)$$

where $\sigma_q^2 = (\sigma_r/2Be)^2$ is the circuit-noise parameter discussed in Sec. 17.5C. The principal advantage of the heterodyne system is now apparent. For strong light or low circuit noise ($\bar{m} \gg \sigma_q^2$), the direct-detection result is $\text{SNR} = \bar{m}$. The heterodyne receiver, which yields $\text{SNR} = 2\bar{m}$, offers a factor-of-2 improvement (3-dB advantage). But for weak light (or large circuit noise) the advantage can be even more substantial, since the heterodyne receiver has $\text{SNR} = 2\bar{m}$, whereas the SNR of the direct-detection receiver is reduced by circuit noise to $\text{SNR} = \bar{m}/(1 + \sigma_q^2/\bar{m})$.

The performance of a direct-detection *avalanche* photodiode receiver is also inferior to that of a heterodyne photodiode receiver. In accordance with (17.5-32), the SNR obtained when the APD gain is sufficiently large to overcome circuit noise is

$$\text{SNR} = \frac{\bar{m}}{F},$$

where F is the APD excess noise factor ($F > 1$). Therefore, even a noiseless APD receiver ($F = 1$) is a factor of 2 inferior to the heterodyne receiver.

Advantages of Heterodyne Receivers

In comparison with the direct-detection receiver, the heterodyne receiver has the following advantages:

- It is capable of measuring the optical phase and frequency.
- It permits the use of wavelength-division multiplexing (WDM) with smaller channel spacing (≈ 100 MHz). In conventional direct-detection systems the channel spacing is of the order of 100 GHz.
- It permits the use of electronic equalization to compensate for pulse broadening in the fiber. Pulse broadening is a result of the dephasing of the different wavelength/frequency components because of differences in group velocities. Since the receiver monitors the phase, this dephasing may be removed by proper electronic filtering.
- By use of a strong reference field, the heterodyne receiver has an inherent noiseless gain conversion factor that effectively amplifies the signal above the circuit noise level.
- It provides a 3-dB advantage over even the noiseless direct-detection receiver.
- It is insensitive to unwanted background light with which the local oscillator does not mix. Heterodyning is one of the few ways of attaining photon-noise-limited detection in the infrared, where background noise is so prevalent.

The cost of these advantages is an increase in the system's complexity since heterodyning requires a stable local oscillator, an optical coupler in which the mixed fields are precisely aligned, and complex circuits for phase locking.

C. Performance of the Digital Heterodyne Receiver

In this section the performance and sensitivity of a digital coherent communication system are determined in the cases of amplitude and phase modulation.

On-Off Keying (OOK) Homodyne System

Consider an on-off keying (OOK) system transmitting data at a rate B_0 bits/s and using a homodyne receiver. Bits “1” and “0” are represented by the presence and absence of the signal \bar{i}_s during the bit time $T = 1/B_0$, respectively. Assuming that $\varphi_s = \varphi_L = 0$ and $\nu_I = \nu_s - \nu_L = 0$, the measured current has the following means and variances obtained from (22.5-6a) and (22.5-6b):

$$\begin{aligned} \text{mean } \mu_1 &\approx \bar{i}_L + 2(\bar{i}_L \bar{i}_s)^{1/2}, & \text{variance } \sigma_1^2 &\approx 2\bar{i}_L eB & \text{for bit “1”} \\ \text{mean } \mu_0 &\approx \bar{i}_L, & \text{variance } \sigma_0^2 &\approx 2\bar{i}_L eB & \text{for bit “0.”} \end{aligned} \quad (22.5-10)$$

The receiver bandwidth $B = B_0/2$ since the bit time $T = 1/B_0$ is the sampling time $1/2B$ for a signal of bandwidth B .

The performance of the binary communication system under the Gaussian approximation has been discussed in Sec. 22.4. The bit error rate is given by (22.4-7), where

$$Q = \frac{\mu_1 - \mu_0}{\sigma_1 + \sigma_0} = \left(\frac{\bar{i}_s}{2eB} \right)^{1/2} = \bar{m}^{1/2}, \quad (22.5-11)$$

and $\bar{m} = \bar{i}_s/2eB$ is the mean number of detected photoelectrons in bit 1. For a bit error rate $\text{BER} = 10^{-9}$, $Q \approx 6$ and therefore $\bar{m} = 36$, corresponding to a receiver sensitivity $\bar{m}_a = \frac{1}{2}\bar{m} = 18$ photoelectrons per bit (averaged over both bits).

Phase-Shift-Keying (PSK) Homodyne System

Here bits “1” and “0” are represented by a phase shift $\varphi_s = 0$ and π , respectively. Assuming that $\varphi_L = 0$, the means and variances of the photocurrent for bits “1” and “0” are, from (22.5-6),

$$\begin{aligned} \text{mean } \mu_1 &= \bar{i}_L + 2(\bar{i}_L \bar{i}_s)^{1/2}, & \text{variance } \sigma_1^2 &= 2e\bar{i}_L B & \text{for bit “1”} \\ \text{mean } \mu_0 &= \bar{i}_L - 2(\bar{i}_L \bar{i}_s)^{1/2}, & \text{variance } \sigma_0^2 &= 2e\bar{i}_L B & \text{for bit “0”} \end{aligned}$$

and therefore

$$Q = \frac{\mu_1 - \mu_0}{\sigma_1 + \sigma_0} = 2 \left(\frac{\bar{i}_s}{2eB} \right)^{1/2} = 2(\bar{m})^{1/2}. \quad (22.5-12)$$

For a $\text{BER} = 10^{-9}$, $Q = 6$, from which $\bar{m} = 9$. Since *each* of the two bits must carry an average of nine photoelectrons in this case, the average number of photoelectrons per bit is $\bar{m}_a = \bar{m} = 9$. It follows that the receiver sensitivity is 9 photoelectrons/bit. The PSK homodyne receiver is twice as sensitive as the OOK homodyne receiver because it requires half the number of photoelectrons.

Comparison

The sensitivity of the heterodyne digital receiver can be determined by following a similar analysis. Table 22.5-1 lists the receiver sensitivities of several digital modulation systems, assuming $\eta = 1$. Although it appears that the direct-detection OOK system has about the same performance as the best coherent system (homodyne PSK), in

TABLE 22.5-1 Receiver Sensitivity of Different Receivers and Modulation Systems under Ideal Conditions (Photons per Bit)

	Direct Detection	Homodyne	Heterodyne
OOK	10	18	36
PSK	—	9	18
FSK	—	—	36

practice this is not so. In the homodyne system, circuit noise is overcome, whereas in the direct-detection system, circuit noise cannot be ignored, unless an APD is used. When an APD is used in a direct-detection receiver, circuit noise is overcome, but the APD gain noise raises the receiver sensitivity from 10 to at least $10F$, where F is the excess-noise factor. Direct-detection systems would have performance comparable to coherent-detection systems if a perfect APD with $F = 1$ (no excess noise) were available.

D. Coherent Systems

An essential condition for the proper mixing of the local oscillator field and the received optical field is that they must be locked in phase, be parallel, and have the same polarization in order to permit interference to take place. This places stringent requirements on the two lasers and on the fiber. The lasers must be single-frequency and have minimal phase and intensity fluctuations. The local oscillator is phase-locked to the received optical field by means of a control system that adjusts the phase and frequency of the local oscillator adaptively (using a phase-locked loop). The fiber must be single-mode (to avoid modal noise). The fiber must also be polarization-maintaining, or the receiver must contain an adaptive polarization-compensation system.

A schematic diagram of a coherent fiber-optic communication system using two lasers and phase modulation is shown in Fig. 22.5-3. The local oscillator field is mixed with the received optical field using an optical directional coupler. One branch of the coupler output contains the sum of the two optical fields and the other branch contains the difference. Using (22.5-2), the detected currents

$$\bar{i}_{\pm} = \bar{i}_s + \bar{i}_L \pm 2(\bar{i}_s \bar{i}_L)^{1/2} \cos[2\pi\nu_L t + (\varphi_s - \varphi_L)]$$

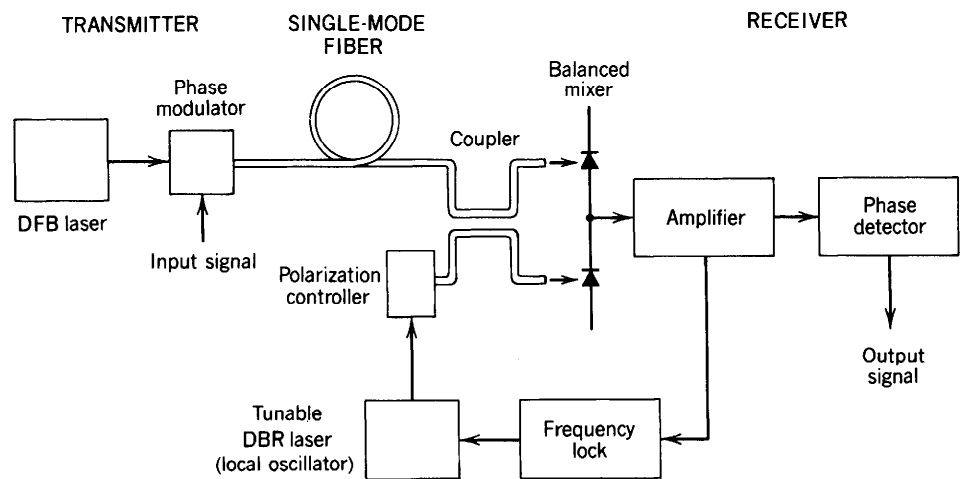


Figure 22.5-3 Coherent fiber-optic communication system.

are subtracted electronically, yielding $4(\hat{i}_s \hat{i}_L)^{1/2} \cos[2\pi\nu_f t + (\varphi_s - \varphi_L)]$, which is demodulated to recover the message. This type of coherent receiver is known as a **balanced mixer**. It has the advantage of canceling out intensity fluctuations of the local oscillator. A number of coherent fiber-optic communication systems have been implemented at $\lambda_o = 1.55 \mu\text{m}$ (where fiber attenuation is minimal) with bit-rate-distance products matching theoretical expectations.

One example is provided by a system operating at a bit rate $\approx 4 \text{ Gb/s}$. A DFB laser with a 15-MHz CW linewidth was directly modulated in an FSK signal format. The local oscillator was a tunable DBR laser (see Sec. 16.3E). This system exhibited a receiver sensitivity ≈ 190 photons/bit and was used for transmission over a 160-km length of fiber.

READING LIST

See also the reading lists in Chapters 7, 8, 16, 17, and 21.

Books

- T. Li, ed., *Optical Fiber Data Transmission*, Academic Press, Boston, 1991.
- H. B. Killen, *Fiber Optic Communications*, Prentice Hall, Englewood Cliffs, NJ, 1991.
- P. K. Cheo, *Fiber Optics and Optoelectronics*, Prentice Hall, Englewood Cliffs, NJ, 1990.
- T. C. Edwards, *Fiber-Optic Systems: Network Applications*, Wiley, New York, 1989.
- J. C. A. Chaimowicz, *Lightwave Technology*, Butterworths, Boston, 1989.
- C. Lin, ed., *Optoelectronic Technology and Lightwave Communications Systems*, Van Nostrand Reinhold, New York, 1989.
- S. E. Miller and I. P. Kaminow, eds., *Optical Fiber Telecommunications II*, Academic Press, New York, 1988.
- S. Karp, R. Gagliardi, S. E. Moran, and A. Holland, *Optical Channels: Fibers, Clouds, Water, and the Atmosphere*, Plenum Press, New York, 1988.
- W. B. Jones, Jr., *Introduction to Optical Fiber Communication Systems*, Holt, Rinehart and Winston, New York, 1988.
- J. C. Palais, *Fiber Optic Communications*, Prentice Hall, Englewood Cliffs, NJ, 2nd ed. 1988.
- T. Okoshi and K. Kikuchi, *Coherent Optical Fiber Communications*, Kluwer, Boston, 1988.
- C. K. Kao, *Optical Fibre*, Peter Peregrinus, London, 1988.
- C. D. Chaffee, *The Rewiring of America: The Fiber Optics Revolution*, Academic Press, Boston, 1988.
- H. F. Taylor, ed., *Advances in Fiber Optics Communications*, Artech House, Norwood, MA, 1988.
- S. Geckeler, *Optical Fiber Transmission Systems*, Artech House, Norwood, MA, 1987.
- G. Mahlke and P. Gössing, *Fiber Optic Cables*, Wiley, New York, 1987.
- P. K. Runge and P. R. Trischitta, eds., *Undersea Lightwave Communications*, IEEE Press, New York, 1986.
- C. Baack, ed., *Optical Wideband Transmission Systems*, CRC Press, Boca Raton, FL, 1986.
- S. D. Personick, *Fiber Optics: Technology and Applications*, Plenum Press, New York, 1985.
- D. G. Baker, *Fiber Optic Design and Applications*, Reston Publishing, Reston, VA, 1985.
- J. M. Senior, *Optical Fiber Communications*, Prentice-Hall, Englewood Cliffs, NJ, 1985.
- J. Gowar, *Optical Communication Systems*, Prentice-Hall, Englewood Cliffs, NJ, 1984.
- B. Culshaw, *Optical Fibre Sensing and Signal Processing*, Peter Peregrinus, London, 1984.
- J. C. Daly, ed., *Fiber Optics*, CRC Press, Boca Raton, FL, 1984.
- A. H. Cherin, *An Introduction to Optical Fibers*, McGraw-Hill, New York, 1983.
- G. Keiser, *Optical Fiber Communications*, McGraw-Hill, New York, 1983.

- D. J. Morris, *Pulse Code Formats for Fiber Optical Data Communication: Basic Principles and Applications*, Marcel Dekker, New York, 1983.
- H. F. Taylor, ed., *Fiber Optics Communications*, Artech House, Dedham, MA, 1983.
- Y. Suematsu and K. Iga, *Introduction to Optical Fiber Communications*, Wiley, New York, 1982.
- H. Kressel, ed., *Semiconductor Devices for Optical Communication*, Springer-Verlag, New York, 2nd ed. 1982.
- T. Okoshi, *Optical Fibers*, Academic Press, New York, 1982.
- C. K. Kao, *Optical Fiber Systems*, McGraw-Hill, New York, 1982.
- S. D. Personick, *Optical Fiber Transmission Systems*, Plenum Press, New York, 1981.
- M. K. Barnoski, ed., *Fundamentals of Optical Fiber Communications*, Academic Press, New York, 2nd ed. 1981.
- A. B. Sharma, S. J. Halme, and M. M. Butusov, *Optical Fiber Systems and Their Components*, Springer-Verlag, Berlin, 1981.
- CSELT (Centro Studi e Laboratori Telecomunicazioni), *Optical Fibre Communications*, McGraw-Hill, New York, 1981.
- C. P. Sandbank, ed., *Optical Fibre Communication Systems*, Wiley, New York, 1980.
- M. J. Howes and D. V. Morgan, eds., *Optical Fibre Communications*, Wiley, New York, 1980.
- J. E. Midwinter, *Optical Fibers for Transmission*, Wiley, New York, 1979.
- S. E. Miller and A. G. Chynoweth, *Optical Fiber Telecommunications*, Academic Press, New York, 1979.
- B. Saleh, *Photoelectron Statistics with Applications to Spectroscopy and Optical Communication*, Springer-Verlag, Berlin, 1978.
- G. R. Elion and H. A. Elion, *Fiber Optics in Communication Systems*, Marcel Dekker, New York, 1978.
- R. O. Harger, *Optical Communication Theory*, Dowden, Hutchinson & Ross, Stroudsburg, PA, 1977.
- R. M. Gagliardi and S. Karp, *Optical Communications*, Wiley, New York, 1976.
- W. K. Pratt, *Laser Communication Systems*, Wiley, New York, 1969.

Special Journal Issues

- Special issue on optical fiber communication, *Optics and Photonics News*, vol. 1, no. 11, 1990.
- Special issue on wide-band optical transmission technology and systems, *Journal of Lightwave Technology*, vol. LT-6, no. 11, 1988.
- Special issue on fiber optic local and metropolitan area networks, *IEEE Journal of Selected Areas in Communications*, vol. SAC-6, no. 6, 1988.
- Special issue on factors affecting data transmission quality, *Journal of Lightwave Technology*, vol. LT-6, no. 5, 1988.
- Special issue on high speed technology for lightwave applications, *Journal of Lightwave Technology*, vol. LT-5, no. 10, 1987.
- Special issue on coherent communications, *Journal of Lightwave Technology*, vol. LT-5, no. 4, 1987.
- Special issue on fiber optic systems for terrestrial applications, *IEEE Journal of Selected Areas in Communications*, vol. SAC-4, no. 9, 1986.
- Joint special issue on lightwave devices and subsystems, *Journal of Lightwave Technology*, vol. LT-3, no. 6; and *IEEE Transactions on Election Devices*, vol. ED-32, no. 12, 1985.
- Special issue on fiber optics for local communications, *IEEE Journal of Selected Areas in Communications*, vol. SAC-3, no. 6, 1985.
- Joint special issue on undersea lightwave communications, *Journal of Lightwave Technology*, vol. LT-2, no. 6; and *IEEE Journal of Selected Areas in Communications*, vol. SAC-2, no. 6, 1984.
- Special issue on fiber optic systems, *IEEE Journal of Selected Areas in Communications*, vol. SAC-1, no. 3, 1983.
- Special issue on communications aspects of single-mode optical fiber and integrated optical technology, *IEEE Journal of Quantum Electronics*, vol. QE-17, no. 6, 1981.

- Special issue on optical-fiber communications, *Proceedings of the IEEE*, vol. 68, no. 10, 1980.
- Special issue on quantum-electronic devices for optical-fiber communications, *IEEE Journal of Quantum Electronics*, vol. QE-14, no. 11, 1978.
- Special issue on optical communication, *Proceedings of the IEEE*, vol. 58, no. 10, 1970.

Articles

- E. Desurvire, Erbium-Doped Fiber Amplifiers for New Generations of Optical Communication Systems, *Optics & Photonics News*, vol. 2, no. 1, pp. 6–11, 1991.
- K. Nakagawa and S. Shimada, Optical Amplifiers in Future Optical Communication Systems, *IEEE Lightwave Communication Systems Magazine*, vol. 1, no. 4, pp. 57–62, 1990.
- P. E. Green and R. Ramaswami, Direct Detection Lightwave Systems: Why Pay More?, *IEEE Lightwave Communication Systems Magazine*, vol. 1, no. 4, pp. 36–49, 1990.
- R. E. Wagner and R. A. Linke, Heterodyne Lightwave Systems: Moving Towards Commercial Use, *IEEE Lightwave Communication Systems Magazine*, vol. 1, no. 4, pp. 28–35, 1990.
- J. A. Jay and E. M. Hopiavuori, Dispersion-Shifted Fiber Hits its Stride, *Photonics Spectra*, vol. 24, no. 9, pp. 153–158, 1990.
- M. G. Drexhage and C. T. Moynihan, Infrared Optical Fibers, *Scientific American*, vol. 259, no. 5, pp. 110–116, 1988.
- R. A. Linke and A. H. Gnauck, High-Capacity Coherent Lightwave Systems, *Journal of Lightwave Technology*, vol. 6, pp. 1750–1769, 1988.
- S. F. Jacobs, Optical Heterodyne (Coherent) Detection, *American Journal of Physics*, vol. 56, pp. 235–245, 1988.
- K. Nosu, Advanced Coherent Lightwave Technologies, *IEEE Communications Magazine*, vol. 26, no. 2, pp. 15–21, 1988.
- W. J. Tomlinson and C. A. Brackett, Telecommunications Applications of Integrated Optics and Optoelectronics, *Proceedings of the IEEE*, vol. 75, pp. 1512–1523, 1987.
- R. A. Linke and P. S. Henry, Coherent Optical Detection: A Thousand Calls on One Circuit, *IEEE Spectrum*, vol. 24, no. 2, pp. 52–57, 1987.
- S. R. Nagel, Optical Fiber—the Expanding Medium, *IEEE Communications Magazine*, vol. 25, no. 4, pp. 33–43, 1987.
- T. Li, Advances in Lightwave Systems Research, *AT & T Technical Journal*, vol. 66, no. 1, pp. 5–18, 1987.
- H. Kogelnik, High-Speed Lightwave Transmission in Optical Fibers, *Science*, vol. 228, pp. 1043–1048, 1985.
- M. C. Teich, Laser Heterodyning, *Optica Acta (Journal of Modern Optics)*, vol. 32, pp. 1015–1021, 1985.
- P. S. Henry, Lightwave Primer, *IEEE Journal of Quantum Electronics*, vol. QE-21, pp. 1862–1879, 1985.
- I. W. Stanley, A Tutorial Review of Techniques for Coherent Optical Fiber Transmission Systems, *IEEE Communications Magazine*, vol. 23, no. 8, pp. 37–53, 1985.
- T. Li, Lightwave Telecommunication, *Physics Today*, vol. 38, no. 5, pp. 24–31, 1985.
- J. D. Crow, Computer Applications for Fiber Optics, *IEEE Communications Magazine*, vol. 23, no. 2, pp. 16–20, 1985.
- Y. Suematsu, Long-Wavelength Optical Fiber Communication, *Proceedings of the IEEE*, vol. 71, pp. 692–721, 1983.

PROBLEMS

- 22.1-1 **Fiber-Optic Systems.** Discuss the validity of each of the following statements and indicate the conditions under which your conclusion is applicable.
- (a) The wavelength $\lambda_o = 1.3 \mu\text{m}$ is preferred to $\lambda_o = 0.87 \mu\text{m}$ for all fiber-optic communication systems.

- (b) The wavelength $\lambda_o = 1.55 \mu\text{m}$ is preferred to $\lambda_o = 1.3$ for all fiber-optic communication systems.
- (c) Single-mode fibers are superior to multimode fibers because they have lower attenuation coefficients.
- (d) There is no pulse spreading at $\lambda_o \approx 1.312 \mu\text{m}$ in silica glass fibers.
- (e) Compound semiconductor devices are required for fiber-optic communication systems.
- (f) APDs are noisier than *p-i-n* photodiodes and are therefore not useful for fiber-optic systems.

22.1-2 Components for Fiber-Optic Systems. The design of a fiber-optic communication system involves many choices, some of which are shown in Table 22.1-2 on page 886. Make reasonable choices for each of the applications listed below. More than one answer may be correct. Some choices, however, are incompatible.

- (a) A transoceanic cable carrying data at a 100-Mb/s rate with 100-km repeater spacings.
- (b) A 1-m cable transmitting analog data from a sensor at 1 kHz.
- (c) A link for a computer local-area network operating at 500 Mb/s.
- (d) A 1-km data link operating at 100 Mb/s with $\pm 50^\circ\text{C}$ temperature variations.

22.3-1 Performance of a Plastic Fiber Link. A short-distance low-data-rate communication system uses a plastic fiber with attenuation coefficient 0.5 dB/m, an LED generating 1 mW at a wavelength of $0.87 \mu\text{m}$, and a photodiode with receiver sensitivity -20 dBm . Assuming a power loss of 3 dB each at the input and output couplers, determine the maximum length of the link. Assume that the data rate is sufficiently low so that dispersion effects play no role.

22.3-2 Power Budget. A fiber-optic communication link is designed for operation at 10 Mb/s. The source is a 1-mW AlGaAs diode laser operating at $0.87 \mu\text{m}$. The fiber is made of 1-km segments each with attenuation 3.5 dB/km. Connectors between segments have a loss of 2 dB each and input and output couplers each introduce a loss of 2 dB. The safety margin is 6 dB. Two receivers are available, a Si *p-i-n* photodiode receiver with sensitivity 5000 photons per bit, and a Si APD with sensitivity 125 photons per bit. Determine the maximum length of the link for each receiver.

22.4-1 Dependence of Receiver Sensitivity on Wavelength. The receiver sensitivity of an ideal receiver (with unity quantum efficiency and no circuit noise) operating at a wavelength $0.87 \mu\text{m}$ is -76 dBm . What is the sensitivity at $1.3 \mu\text{m}$ if the receiver is operated at the same data rate?

22.4-2 Bit Error Rates. A quantum-limited *p-i-n* photodiode (no noise other than photon noise) of quantum efficiency $\eta = 1$ mistakes a present $\lambda_o = 0.87 \mu\text{m}$ optical signal of power P (bit 1) for an absent signal (bit 0) with probability 10^{-10} . What is the probability of error under each of the following new conditions?

- (a) The wavelength is $\lambda_o = 1.3 \mu\text{m}$.
- (b) Original conditions, but now the power is doubled.
- (c) Original conditions, but the efficiency is now $\eta = 0.5$.
- (d) Original conditions, but an ideal APD with $\eta = 1$ and gain $G = 100$ (no gain noise) is used.
- (e) As in part (d), but the APD has an excess noise factor $F = 2$ instead.

22.4-3 Sensitivity of an AM Receiver. A detector with responsivity \mathfrak{R} (A/W), bandwidth B , and negligible circuit noise, measures a modulated optical power $P(t) = P_0 + P_s \cos(2\pi ft)$, with $f < B$. If $P_0 \gg P_s$, derive an expression for the minimum modulation power P_s that is measurable with signal-to-noise ratio $\text{SNR}_0 = 30 \text{ dB}$. What is the effect of the background power P_0 on the minimum observable signal P_s ?

- 22.4-4 **Maximum Length of an Analog Link.** A fiber-optic communication link uses intensity modulation to transmit data at a bandwidth $B = 10$ MHz and signal-to-noise ratio of 40 dB. The source is a $\lambda_o = 0.87 \mu\text{m}$ light-emitting diode producing $100 \mu\text{W}$ average power with maximum modulation index of 0.5. The fiber is a multimode step-index fiber with attenuation coefficient 2.5 dB/km . The detector is an avalanche photodiode with mean gain $\bar{G} = 100$, excess noise factor $F = 5$, and responsivity of 0.5 A/W (not including the gain). Assuming that the circuit noise is negligible, calculate the optical power sensitivity of the receiver and the attenuation-limited maximum length L of the fiber.
- 22.4-5 **Sensitivity of a Photon-Counting Receiver.** A photodetector of quantum efficiency $\eta = 0.5$ counts photoelectrons received in successive time intervals of duration $T = 1 \mu\text{s}$. Determine the receiver sensitivity (mean number of photons required to achieve $\text{SNR} = 10^3$) assuming a Poisson photon-number distribution. Assuming that the wavelength of the light is $\lambda_o = 0.87 \mu\text{m}$, what is the corresponding optical power? If this optical power is received, what is the probability that the detector registers zero counts?